

The INTEGRAL/IBIS AGN catalogue I: X-ray absorption properties versus optical classification

A. Malizia,^{1*} L. Bassani,¹ A. Bazzano,² A. J. Bird,³ N. Masetti,¹
F. Panessa,² J. B. Stephen,¹ P. Ubertini²

¹ *INAF/IASF-Bologna, Via P. Gobetti 101, I-40129 Bologna, Italy*

² *INAF/IASF-Roma, Via Fosso del Cavaliere 100, I-00133, Roma, Italy*

³ *School of Physics and Astronomy, University of Southampton, SO17 1BJ, Southampton, UK*

Accepted Received ...; in original form ...

ABSTRACT

In this work we present the most comprehensive INTEGRAL AGN sample. It lists 272 AGN for which we have secure optical identifications, precise optical spectroscopy and measured redshift values plus X-ray spectral information, i.e. 2-10 keV and 20-100 keV fluxes plus column density. Here we mainly use this sample to study the absorption properties of active galaxies, to probe new AGN classes and to test the AGN unification scheme. We find that half (48%) of the sample is absorbed while the fraction of Compton thick AGN is small ($\sim 7\%$). In line with our previous analysis, we have however shown that when the bias towards heavily absorbed objects which are lost if weak and at large distance is removed, as it is possible in the local Universe, the above fractions increase to become 80% and 17%. We also find that absorption is a function of source luminosity, which implies some evolution in the obscuration properties of AGN. Few peculiar classes, so far poorly studied in the hard X-ray band, have been detected and studied for the first time such as 5 XBONG, 5 type 2 QSOs and 11 LINERs. In terms of optical classification, our sample contains 57% of type 1 and 43% of type 2 AGN; this subdivision is similar to that found in X-rays if unabsorbed versus absorbed objects are considered, suggesting that the match between optical and X-ray classification is overall good. Only a small percentage of sources (12%) does not fulfill the expectation of the unified theory as we find 22 type 1 AGN which are absorbed and 10 type 2 AGN which are unabsorbed. Studying in depth these outliers we found that most of the absorbed type 1 AGN have X-ray spectra characterized by either complex or warm/ionized absorption more likely due to ionized gas located in an accretion disk wind or in the biconical structure associated to the central nucleus, therefore unrelated to the toroidal structure. Among 10 type 2 AGN which resulted to be unabsorbed, at most 3-4% is still eligible to be classified as a "true" type 2 AGN.

Key words: catalogues – surveys – gamma-rays: observations – X-rays: observations.

1 INTRODUCTION

Observations of Active Galactic Nuclei (AGN) have revealed that many of them are obscured by material (dust and gas) located within the inner tens of parsecs of the central engine (see e.g. Bianchi et al. 2012 for a review) and intercepted by our line of sight. This obscuring material will influence both the AGN and our observations, and the study of its properties is fundamental for an unbiased understanding of AGN physics. For example obscuration by gas and dust is a key ingredient of the AGN Unified Scheme, which proposes that

type 2 and type 1 AGN are intrinsically the same type of object viewed from different orientation angles (Antonucci 1993): when our line of sight does not intercept any absorbing material the source is classified as a type 1 AGN while in the opposite case, where we see obscuring gas and dust, the source is defined as a type 2 AGN. The absorbing material which determines the two main flavours of active galaxies is most likely a toroidal structure (doughnut like or clumpy) thought to be present in all AGN.

How many objects are absorbed or not and what is the distribution of absorption among all objects are important information for AGN studies. Cosmic X-ray background (CXB) synthesis models, in the context of the AGN Unification the-

* E-mail address: malizia@iasfbo.inaf.it

ory and based on a combination of absorbed and unabsorbed AGN, have been quite successful in reproducing the overall broadband spectral shape of the observed background (Gilli et al. 2007), but they need accurate observational information on the absorption parameter. Absorbed sources constitute also an important ingredient for the IR and the sub-mm backgrounds, where most of the absorbed radiation is re-emitted by dust (e.g. Fabian & Iwasawa 1999).

Many important issues related to the population of absorbed AGN are still to be understood, like the number of type 2 QSO, the nature of the X-ray bright optical normal galaxies (XBONG), the role of LINERs and the relationship between optical absorption and X-ray obscuration.

Because of the effect it may have on observations, absorption can be problematic for surveys performed at various wavebands and this is the main motivation for performing AGN surveys above 20 keV.

In this work we have gathered a large number (272) of AGN detected by INTEGRAL, collected their optical classification and X-ray column density measurements in order to be able to study the absorption properties in a large sample of hard X-ray selected AGN, explore the nature of absorption in XBONGs, type 2 QSO's and LINERs and finally compare the optical classification with the X-ray absorption as a tool to test the AGN Unification Theory.

It is worth noting that these studies have often been performed employing samples of AGN observed in the soft (below 20 keV) X-ray band and only recently with the advent of enough AGN being detected at higher X-ray energies have similar studies been attempted for the first time.

The paper is organized as follows: the INTEGRAL AGN catalogue is presented in section 2, the study of absorption properties including a discussion on the fraction of heavily absorbed objects is reported in section 3, peculiar objects belonging to the LINER, XBONG and type 2 QSO classes are presented in section 4. In section 5 the optical classification versus X-ray absorption has been treated and in subsections 5.1 and 5.2 the absorbed type 1 AGN and unabsorbed type 2 AGN have been discussed. The summary and conclusions are drawn in section 6.

2 THE INTEGRAL AGN CATALOGUE

In the 4th INTEGRAL/IBIS survey (Bird et al. 2010) there are 234 objects which have been identified with AGN. To this set of sources, we have then added 38 galaxies listed in the INTEGRAL all-sky survey by Krivonos et al. (2007) updated on the website¹ but not included in the Bird et al. catalogue due to the different sky coverage (see source names in bold in the Appendix). The final dataset presented and discussed in this work therefore comprises 272 AGN (last update March 2011), which represents the most complete view of the INTEGRAL extragalactic sky to date. Although new source identifications/classifications are continuously coming in (e.g. Masetti et al. 2012), they are not considered in the present dataset because they are not properly characterized in X-rays (see below). In the Appendix we present the full catalogue, listing all 272 INTEGRAL AGN together

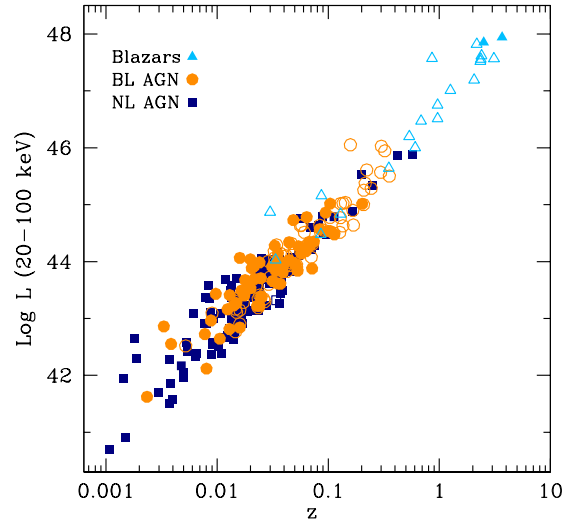


Figure 1. Hard X-ray luminosity vs redshift for all the INTEGRAL AGN sample. Circles are broad line (BL) AGN, squares are narrow line (NL) AGN and triangles are blazars (see section 5 for a more detailed classification). Filled symbols represent objects where intrinsic absorption in excess to the Galactic one has been measured while open symbol refer to sources where there is only an upper limit to the column density, including Galactic values.

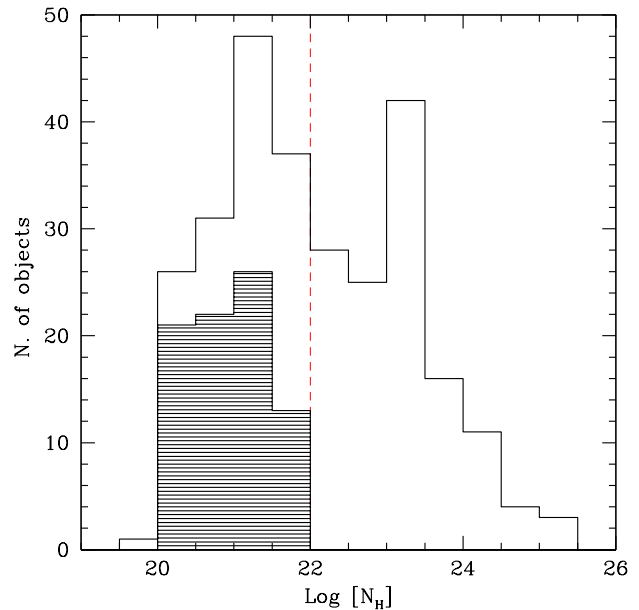


Figure 2. Distribution of column densities in the INTEGRAL AGN. The dashed bins represent upper limit measurements including Galactic values.

¹ <http://hea.iki.rssi.ru/integral/survey/catalog.php>

with their optical coordinates, redshift, class, 20-100 keV flux and X-ray data (2-10 keV flux, column density and reference work from which these data have been taken).

The sample has two great strengths: a) all sources have optical spectra, which means a secure identification and a measured redshift (the only exception is the BL LAC object RX J0137.7+5814 for which no redshift measure is available), and b) all sources have X-ray data available, which provides a measure of the intrinsic absorption in each source. Until recently, 34 sources did not have X-ray (2-10 keV) coverage mainly due to the fact that they are newly discovered AGN; for these sources X-ray data available from the Swift and XMM-Newton archives have been analysed and the results were published by Malizia et al. (2011) except for IGR J04221+4856 which has been recently observed by Swift and the measurements of 2-10 keV flux and column density are reported here for the first time (see table in the Appendix). It is also worth noting that for each source we have verified that the X-ray counterpart of the IBIS object corresponds to the optical identification.

In order to assign to each object the most appropriate optical class, we have searched the literature thoroughly and when possible have also compared the class reported in NED (NASA Extragalactic database) with that listed in the 13th edition of the Veron-Cetty, Veron extragalactic catalogue (2010); a significant number of AGN in the sample have been classified through our own follow up work (Masetti et al. 2012 and references therein). In these cases, we have adopted the classification criteria of Veilleux & Osterbrock (1987) and the line ratio diagnostics of both Ho et al. (1993, 1997) and Kauffmann et al. (2003); for assigning Seyfert subclasses (1.2, 1.5, 1.8, and 1.9), we have used the $H\alpha/[OIII]\lambda 5007$ line flux ratio criterion described in Winkler (1992). We have generally preferred the most recent classification and, in case of conflicting results, we have always checked the optical spectra before assigning the most appropriate optical type.

The overall result is a list of AGN properly characterized at optical, soft and hard X-ray frequencies thus available for population studies.

In figure 1 the whole sample is reported in the classical 20-100 keV luminosity *vs* redshift plot. The luminosities have been calculated for all sources assuming $H_0=71 \text{ km s}^{-1} \text{ Mpc}^{-1}$ and $q_0 = 0$. All AGN have been plotted using three different symbols and following the optical classification (broad line (BL) and narrow (NL) AGN plus blazar); a more detailed analysis of the various optical classes also in terms of absorption, can be found in section 5. From figure 1 it can be estimated that our sensitivity limit is around $1.5 \times 10^{-11} \text{ erg cm}^{-2} \text{ s}^{-1}$. We find that the source redshifts span from 0.0014 to 3.7 with a mean at $z=0.1477$ and a peak in the distribution at $z = 0.015$; while the Log of 20-100 keV luminosities (in erg s^{-1}) ranges from 40.7 to ~ 48 with a mean at around 46, although the peak of the distribution is at 43.9. NGC 4395 (a Seyfert 2) is the closest and least luminous AGN seen by INTEGRAL, while IGR J22517+2218 (a broad line QSO) is the farthest and most luminous one; the former hosts a relatively small central black hole ($M \sim 10^4$ - $10^5 M_\odot$, Filippenko & Ho 2003) while the latter houses a more massive object ($M = 10^9 M_\odot$, De Rosa private communication). In conclusion, the present INTEGRAL sample spans a large range in source parameters and is therefore rep-

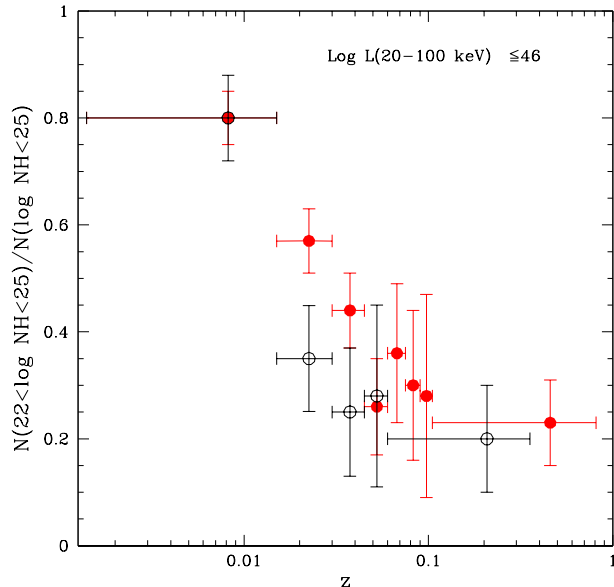


Figure 3. Fraction of absorbed objects compared to the total number of AGN as a function of redshift in the present work (red points) and in the INTEGRAL complete sample of Malizia et al. 2009 (black points).

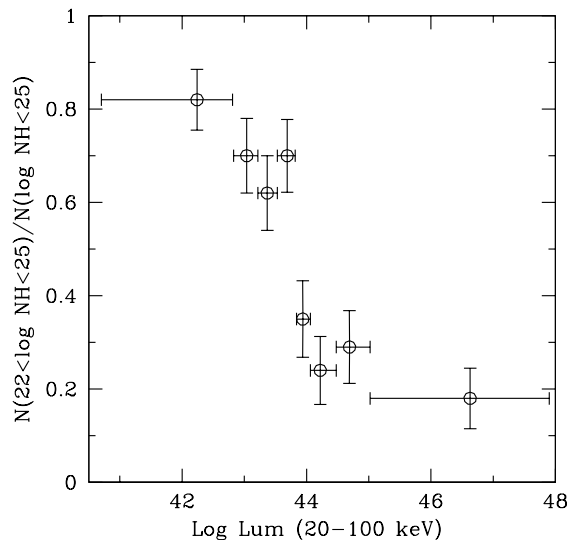


Figure 4. Fraction of absorbed objects compared to the total number of AGN as a function of 20-100 keV luminosity.

representative of the population of AGN selected in the hard X-ray band.

3 ABSORPTION PROPERTIES

Since hard X-ray selected samples provide the most accurate estimate of the fraction of absorbed objects as well as

of Compton thick AGN, we can use the present sample for this purpose. The column density distribution for the entire sample is shown in figure 2. Here and in the following we assume $N_H = 10^{22} \text{ cm}^{-2}$ as the dividing line between absorbed and unabsorbed sources: this is the value conventionally used because it corresponds to a column density sufficiently high to hide the broad line region (BLR, Silverman et al. 2005). It is also worth noting that for a number of objects we did not measure any absorption in excess of the Galactic value and have therefore used the Galactic column density as an upper limit to the source intrinsic absorption. With the assumptions made above the fraction of absorbed objects present in our sample is 48% as can be seen in figure 2.

Within our catalogue we find 15 mildly ($1.5 \times 10^{24} \leq N_H \leq 10^{25} \text{ cm}^{-2}$) and 3 heavily ($N_H \geq 10^{25} \text{ cm}^{-2}$) Compton thick AGN (the full list of objects can be extracted from the table in the Appendix); we therefore estimate the fraction of Compton thick objects to be around $\sim 7\%$, in full agreement with estimates available in the literature (Malizia et al. 2009, Burlon et al. 2011).

Despite the fact that hard X-ray instruments are the least biased in terms of detecting absorbed AGN, they still miss some Compton thick objects, essentially those with weak (intrinsic) fluxes and at large distances. This has been fully discussed by Malizia et al. (2009) and Burlon et al. (2011), who have shown that once the correction for this bias is applied the real intrinsic fraction of Compton-thick AGN is around 20-24%. In particular, in our previous work (Malizia et al. 2009) we have adopted a redshift cut ($z=0.015$ or 60 Mpc) in a complete sample of INTEGRAL AGN in order to remove the bias and to probe, although only locally, the entire AGN population. Following this reasoning and using the present much larger sample of objects, we should be able to expand this study and to confirm our previous hypothesis, having in mind that the present sample is not complete. For comparison with our previous study, we have divided our sample in the same bins of redshift (up to $z=0.57$ considering only the AGN with $\text{Log } L_{20-100 \text{ keV}} \leq 46$) and plotted the fraction of absorbed ($N_H > 10^{22} \text{ cm}^{-2}$) objects compared to the total number of AGN in these bins. The result is shown in figure 3 for the present sample (red points) and for that used in Malizia et al. (2009) (black points).

A number of considerations can be made from this figure: first, the bias is still present as we keep observing a trend of decreasing fraction of absorbed objects as the redshift increases; second, we note that in the first bin the fraction of absorbed objects remains the same as found in our previous analysis: in particular we find that, over the 66 objects present in this bin, 53 (or 80%) have a column density $\geq 10^{22}$ and 11 (or $17\% \pm 3\%$) are Compton thick. Taking into consideration the fact that this is not a complete sample, these results are in close agreement with those found previously and confirm our original suggestion that our survey is able to pick up all AGN, even the most absorbed, but only in the local Universe. Finally, we note that the fraction of absorbed (and Compton thick) AGN has increased in the second bin from 35% to 57% (including 4 Compton thick sources), implying that as the INTEGRAL survey enlarges, we are able to pick up more absorbed objects among those which are distant and faint and therefore lost in previous catalogues. We have also looked for a trend of decreasing

fraction of absorbed AGN with increasing source hard X-ray luminosities. This effect, which is well documented in the X-ray band (Ueda et al. 2003, Hasinger et al. 2005, La Franca et al. 2005, Della Ceca et al. 2008), has also been observed at higher energies (Bassani et al. 2006, Sazonov et al. 2007 and references therein) and is found in our sample too. In figure 4 we show how the fraction of the AGN with $N_H \geq 10^{22} \text{ cm}^{-2}$ in the INTEGRAL sample changes with 20-100 keV luminosity where the width of each bin has been chosen so that the number of objects in each is constant (~ 34). Again, the fraction of absorbed sources is around 80% at low luminosities, decreasing to $\sim 20\%$ at higher luminosities. At the moment it is not possible to discriminate as to whether the redshift effect may have contaminated this result or if it is a direct consequence of the evolution of AGN luminosity function with z , but this issue will be addressed in more detail in a dedicated paper.

Summarizing our results, we conclude that the bias affecting deep hard X-ray surveys of AGN is real but negligible if we deal with objects located in the nearby Universe, where the "true" fraction of absorbed and Compton thick objects can be estimated with some precision at 80% and $\sim 17\%$ respectively.

4 PECULIAR SOURCES

A few interesting classes of objects are now emerging in the INTEGRAL surveys; these are discussed in some detail in the following sub-sections.

4.1 XBONG

One of the most interesting findings of recent soft X-ray surveys is the existence of XBONGs, i.e. X-ray Bright Optically Normal Galaxies (Comastri et al. 2002). These sources are characterized by an X-ray luminosity of 10^{43} - $10^{44} \text{ erg s}^{-1}$ but are optically dull, i.e. they are hosted by normal galaxies whose optical spectra show no emission lines. Different interpretations have been suggested to explain these unusual properties (Trump et al. 2009) including: heavy obscuration by gas covering almost 4π of the nuclear source; a Radiatively Inefficient Accretion Flow (RIAF) which provides a featureless hard X-ray spectrum and negligible emission in the optical and UV bands; and finally dilution of nuclear emission from the host galaxy starlight which prevents the detection of the AGN optical spectrum (Moran et al. 2002). Although these explanations provide a good description of the observed properties of a few objects, the nature of XBONGs is still the subject of debate and recent studies suggest that they could be a mixed bag of different source typologies (Civano et al. 2007).

In the present sample of INTEGRAL AGN there are 5 objects classified as XBONG (see table in the Appendix); all 5 are heavily absorbed in X-rays ($\text{Log } N_H$ from ~ 23 up to $\geq 24 \text{ cm}^{-2}$) and quite bright ($L_{20-100 \text{ keV}}$ in the range 6×10^{42} - $6 \times 10^{44} \text{ erg s}^{-1}$). Clearly, option one is a viable explanation to account for their properties, while it is difficult to reconcile a RIAF accretion model with the X-ray brightness of our objects. We also note that 4 out of 5 sources are optically very bright as they are listed in the USNO B1 catalogue with $R \leq 10.3$; the only exception is IGR J17009+3559

which has $R=14.4$ but is also the XBONG with the highest redshift ($z=0.13$). This suggests that the dilution hypothesis (bright galaxy host) combined with heavy obscuration may be the explanation for the peculiar optical classification of our objects.

4.2 Type 2 QSO

Type 2 QSO are the high redshift/high luminosity counterparts of local Seyfert 2 galaxies. They play an important role in our understanding of the Universe as their existence in considerable numbers is needed for the synthesis of the X-ray background (Gilli et al. 2007). They are also important objects in the subject of the evolution of absorption with intrinsic luminosity and/or redshift; this is an issue which is still matter of intensive debate, but potentially very important for the influence that it can have on many astrophysical issues.

Despite much effort put into their search/quest, very few type 2 QSO have so far been found especially at very high redshifts. They are hard to discover because a significant fraction of their emitted power is absorbed by an optically thick torus and, since they are distant/faint, they are missed by most surveys; in particular, the lack of emission lines over a wide wavelength range hampers their identification in the optical. Hard X-ray surveys are ideally suited for this purpose as they can penetrate the torus in most objects. The definition of type 2 QSO is somewhat arbitrary and depends on the waveband used to find them. In X-rays the definition first introduced by Mainieri et al. (2002) is generally adopted: a type 2 QSO has to have an intrinsic X-ray luminosity of $L > 10^{44}$ erg s $^{-1}$ (0.5-10 keV) and an absorbing hydrogen column density of $N_H > 10^{22}$ cm $^{-2}$. Unfortunately, we do not have 0.5-10 keV luminosity information for all our objects, but can adopt the 2-10 keV band as a measure of the X-ray brightness and the same threshold in luminosity ($> 10^{44}$ erg s $^{-1}$) and column density ($N_H > 10^{22}$ cm $^{-2}$) used by Mainieri et al. (2002).

We have 12 sources fulfilling the above criteria; however 4 of them are local Seyferts ($z < 0.1$) and cannot be considered as type 2 QSO while 2 of them, PKS 1830-211 and IGR J22517+2218 are high redshift blazars in which the high column density measured may not be related to the toroidal structure implied by the AGN unified theory. PKS 1830-211 ($z = 2.507$) is a complicated system, gravitationally lensed by an intervening galaxy at $z = 0.89$. The observed flattening in the X-ray spectrum at low energies has been interpreted in other ways: either as absorption coming from the lensing galaxy, or due to a change in the source spectral shape related to its blazar nature (Zhang et al. 2008). This last interpretation has also been used in the case of the other absorbed blazar IGR J22517+2218 (Bassani et al. 2007). The other source to explain is IGR J10147-6354, classified as a Seyfert 1.2 at $z=0.2$, where the absorption, as well as in other type 1 AGN, is less easy to understand and will be the subject of an in-depth analysis in section 5.

We are left with 5 objects which display evident narrow emission lines in their optical spectra and therefore qualify to be type 2 QSO: IGR J00465-4005, SWIFT J0216.3+5128, IGR J09523-6231, IGR J12288+0052 and IGR J23524+5842. Only IGR J09523-6231 is a type 1.9 AGN implying that a weak broad H α emission line is present in its

optical spectrum. The 2-10 keV luminosity of these objects goes from 3.6×10^{44} erg s $^{-1}$ to 5.6×10^{45} erg s $^{-1}$ while in the 20-100 keV band ranges from 7.6×10^{44} erg s $^{-1}$ to 7.8×10^{45} erg s $^{-1}$. The maximum absorption is measured in IGR J00465-4005 with $N_H \sim 2.4 \times 10^{23}$ cm $^{-2}$ (Landi et al. 2010a). Despite early indications that IGR J12288+0052 could be a Compton thick AGN (Vignali et al. 2010) we find that it is only moderately absorbed (Fiocchi et al. 2010, but see considerations in section 5.2); it is also the source at the highest redshift (0.5756) within this group.

Type 2 QSO constitute therefore a small fraction (2%) of the entire AGN population selected in the hard X-ray band; they are outnumbered by type 1 QSO implying that are either more rare or more difficult to find.

Finally, type 2 QSO have often been associated with very red objects and some authors (Gandhi et al. 2004; Severgnini et al. 2005) have even suggested a connection with ERO (Extremely Red Objects). ERO are characterized as having R-K colour > 5 (Severgnini et al. 2005 and references therein). We have collected this information for 4 out of 5 sources and found that R-K is in the range 2.3-5.6; only IGR J12288+0052 is marginally compatible with being a ERO but its R-K value is only an upper limit. We can therefore conclude that probably none of our sources qualifies to be an ERO .

4.3 LINERs

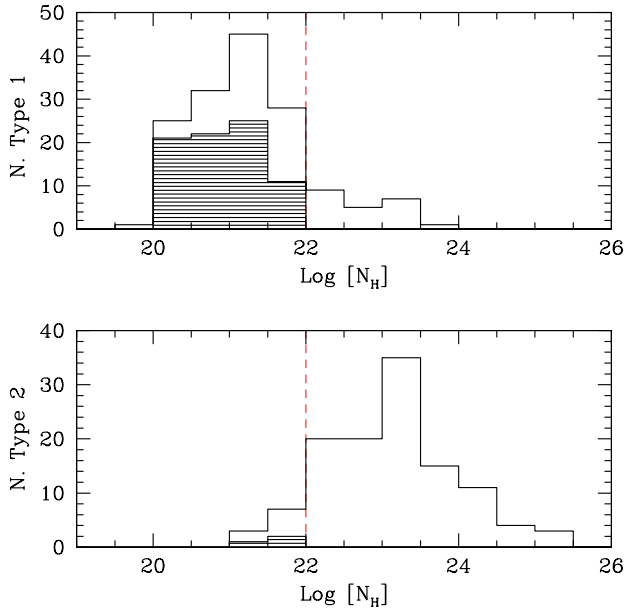
Low-ionization nuclear emission regions (LINERs) were identified as a class of galaxies by Heckman (1980) based on the relative intensities of their oxygen emission lines. Suggestions for the ultimate power source of these objects include (1) a weak active galactic nucleus harboring an accreting, supermassive black hole, (2) hot stars (either young or old) and (3) shocks. Recent radio, UV, and X-ray surveys at high spatial resolution, mid-IR spectroscopy, and variability studies have uncovered weak AGN in the majority of LINERs studied so far, suggesting that they make up a large (perhaps the largest) subset of all AGN (Eracleous et al. 2010). Furthermore, as suggested by Ho (1999) the detection of broad lines in the optical spectra of many LINERs constitute strong evidence in favour of the AGN interpretation. As Seyfert galaxies, also LINERs can be classified in two classes, 1 and 2, depending on whether or not a broad component in their optical spectra can be seen.

In our sample, a number of objects (11) have LINER features: in the optical diagnostic diagrams used for AGN optical classification, 6 fall at the boundary with Seyfert 2 galaxies and 3 at the boundary with Seyfert 1 galaxies; the first are absorbed in X-rays while the second are not. Two objects lie in the region occupied by "pure" LINERs and are also absorbed in X-rays; both display only narrow lines in their optical spectra. So we conclude that, like Seyfert galaxies, also LINERs come in two flavours: unabsorbed type 1 and absorbed type 2. Given their high X-ray luminosities, it is almost certain that all of these objects are powered by AGN, although their 20-100 keV mean luminosity ($\sim 1.7 \times 10^{43}$ erg s $^{-1}$) is slightly lower than that of Seyfert galaxies ($\sim 5.5 \times 10^{43}$ erg s $^{-1}$).

Table 1. Optical classification of sources in the INTEGRAL sample.

Class	Spectral type	Number
Type 1 (57%)	Sy 1	46
	Sy1.2	24
	Sy1.5	45
	Sy1/LINER	3
	NLS1	14
	Blazar	22
Type 2 (43%)	Sy 2	69
	Sy1.9	13
	Sy2/LINER	6
	Radio Gal.	1
	XBONG	4 [†]
	LINERs	2
	QSO 2	5
	Compton thick [†]	18
Total		272

[†] all the Compton thick sources are Seyfert 2 but , NGC 1365, which is optically classified as 1.9 and MCG-07-06-018, which is optically classifies as XBONG.

**Figure 5.** Column density distributions in type 1 (up) and type 2 (down). Dashed bins like in figure 2.

5 OPTICAL CLASSIFICATION VERSUS X-RAY ABSORPTION

The optical classification scheme which follows the orientation-based AGN unified model (Antonucci 1993) is expected to be strictly correlated with the X-ray absorption. However, recently quite a few studies have claimed the existence of objects for which optical and X-ray classifications do not match. Although not yet explained physically, it is commonly found in X-ray selected samples that $\sim 10\%$ - 30% of AGN which have only narrow lines in their optical spectra,

suggesting extinction and thus classified as type 2, do not show absorption in their X-ray spectra (e.g. Panessa & Bassani 2002, Tozzi et al. 2006). On the other hand, there are more and more objects optically classified as type 1 which show significant amount of absorption in their X-ray spectra, a feature which is at odds with the presence of broad lines in the optical band (e.g. Garcet et al. 2007, Panessa et al. 2008).

In this section we explore the connection between optical classification and X-ray absorption in the INTEGRAL AGN sample. Before proceeding with this comparison we need however to make some assumptions.

Intermediate subclasses of Seyferts 1.2 and 1.5 are assigned to type 1 AGN, while those belonging to other types (1.8, 1.9) are considered as type 2 objects. Implicit in this, is the assumption that the late intermediate types (1.8, 1.9) are AGN viewed at intermediate inclination angles to the central source, possibly through the "atmosphere" of the dusty torus. In type 2 objects we have also included Cen B, which is a narrow line radio galaxy and also the 5 XBONGs discussed previously; the underlying assumption is that in these AGN both broad and narrow line regions are hidden by gas and dust. Also the 2 "pure" LINERs (MCG+04-26-006 and IGR J19118-1707) have been considered as type 2 AGN, since in their optical spectra only narrow line components are present. 22 objects in the sample are classified as blazars: 8 are BL Lac objects and 14 QSO. The former tend to be closer than the latter. These blazars have all been included in type 1 AGN for the following reasons: a) all those classified as QSO are broad line objects; b) all BL Lac can be interpreted as AGN where a relativistic jet, which is closely aligned to the line of sight to the observer, swamps the broad and narrow line region making the source optical spectrum featureless.

The overall subdivision into optical classes is summarized in Table 1 where we also quote the percentage of type 1 (57%) and of type 2 (43%) objects. These percentages are not very different from those obtained following the X-ray classification: as seen previously 52% of our objects are unabsorbed and 48% are absorbed, suggesting that the AGN unification model generally holds. However, the match is not perfect as we have a number of absorbed type 1 sources as well as a number of unabsorbed type 2 objects. This is clearly visible in the histograms of the column density reported in figure 5 for type 1 (up) and for type 2 objects (down) separately; the line corresponding to $N_H = 10^{22} \text{ cm}^{-2}$ is also plotted in order to immediately see how many sources fall in the forbidden regions (above and below this value for type 1 and 2 objects respectively). This is quantified in Table 2, which provides the AGN subdivision according to both optical and X-ray classifications. There are 240 objects for which the match is as expected; these sources constitute 88% of the sample. The remaining objects, that is 22 type 1 AGN which are absorbed and 10 type 2 AGN which are unabsorbed, make the remaining 12%. In order to verify this correlation and to be able to compare our results with previous studies, the fourfold point correlation coefficient r defined as in Garcet et al. (2007) has been calculated. The use of this coefficient represents a rigorous way to quantify the correlation between the X-ray and optical classifications: when $r=0$ no correlation is observed, while when $r=1$ there is a strict correlation. We found a fourfold coefficient $r=0.77 \pm 0.05$ which indicates

Table 2. Number of sources as a function of the optical (type 1 and type 2) and X-ray (unabsorbed and absorbed) classifications.

	Opt. type 1	Opt. type 2	Total
Unabsorbed	132	10	140 (52%)
Absorbed	22	108	132 (48%)
Tot	154 (57%)	118 (43%)	272

a good agreement between optical and X-ray classification. Such a high correlation value was only found by Caccianiga et al. (2004) for their sample of bright X-ray sources; when samples of weaker sources are used, r becomes much smaller (around 0.3) implying only a mild correlation between optical and X-ray classifications (Garcet et al. 2007). However, as fully discussed by Garcet et al. (2007), this may be due to difficulties in dealing with objects which are weaker or further away.

5.1 Absorbed type 1 AGN

Among type 1 AGN, 22 objects are absorbed including 2 Seyfert 1s, 6 Seyfert 1.2, 10 Seyfert 1.5, 2 NLS1 and 2 blazars, corresponding to $\sim 14\%$ of the entire type 1 AGN population. Using the errors on column density reported in the table in the Appendix, we can define with some precision that the fraction of absorbed type 1 AGN ranges from 12% to 17%. This percentage is greater than the $\sim 11\%$ found by Garcet et al. (2007) in their XMM selected sample. These authors also found that their absorbed type 1 AGN were high X-ray luminosity objects lying at high redshift (typically above $z=1$) giving an indication that this may be a common property at high redshift and luminosity values. This result, which has been recently confirmed by Mateos et al. (2010) and Scott et al. (2011) using 2-10 keV data, is not found in our hard X-ray sources: in fact, although our objects are relatively luminous in X-rays, they are not brighter than other type 1 objects nor lie at higher redshift (see table in the Appendix).

Several interpretations have been suggested in order to explain the nature of absorbed type 1 AGN. For example, Maiolino et al. (2001a) have discussed a sample of nearby AGN whose X-ray spectra show evidence for cold absorption but there was no hint of obscuration in their optical data (hence their classification as type 1). They concluded that the ratio A_V/N_H in these objects is systematically much lower than the Galactic standard value. In a companion paper, Maiolino et al. (2001b) suggested that a dust distribution dominated by large grains in the obscuring torus could explain the low A_V/N_H values obtained. They claim that the formation of large grains is naturally expected in the high density environment characterizing the circumnuclear region of AGN. These large grains make the extinction curve flatter than the Galactic one and thus for a given N_H value a reduced extinction and reddening are observed, compared to the Galactic standard.

An alternative explanation was proposed by Weingartner & Murray (2002): they suggested that the line of sight to these AGN passes through ionized material located just off the torus and/or accretion disk. This material is responsible

for the X-ray absorption, while the optical/infrared extinction occurs in material farther from the nucleus, where the dust may be quite similar to the Galactic dust. The X-ray-absorbing material may be dust-free or may contain large grains that have very small extinction efficiencies in the optical/infrared. This material may be associated with a disk wind, which would originate within the dust sublimation radius (see Murray et al. 1995). In this case, the dust will sublimate and the obscuration/extinction in the optical will be much reduced, even if there is a strong absorption in the X-rays, produced by the ionized gas.

Finally variability, i.e. non simultaneous X-ray and optical observations, could also explain the apparent discrepancy between the optical and X-ray classifications of some type 1 AGN.

In order to study these absorbed type 1 AGN, we analysed in detail the available X-ray data of each object to have more information on the nature of the absorption measured. The 2 absorbed blazars will not be considered in the following discussion since, as showed in section 4.2, in these objects (PKS 1830-211, De Rosa et al. 2005 and IGR J22367-1231, Bassani et al. 2007) the absorption is probably not intrinsic. We have reported in Table 3 the remaining **20** absorbed type 1 AGN, together with their specific optical sub-class, intrinsic dust reddening when available, X-ray column density, type of X-ray absorption (complex or ionized) reported in the literature, satellite used for the X-ray measurement and reference for the type of absorption. The dust reddening expressed as $N_{H_{Opt}}$ has been estimated from the E_{B-V} intrinsic to the source assuming the Cardelli et al. (1989) extinction law and $N_{H_{Opt}} = 2.22 \times 10^{21} A_V$, where $A_V = 3 \times E_{B-V}$ (Zombeck 1990). It is worth noting that in those cases where the absorption was found to be variable or complex the highest N_H value has been preferred.

As evident from a comparison between the optical and X-ray column densities, dust extinction tends to be systematically lower than gas absorption, in agreement with Maiolino et al. (2001a), implying that a non standard dust to gas ratio is a viable explanation for the absorption in our type 1 objects. A more interesting aspect emerging from Table 3 is the fact that many objects have X-ray spectra characterized by either complex (CA) i.e. multi absorption layers of cold material or warm/ionized (WA) absorption. These two models are somehow interchangeable as demonstrated for MKN 6 by Schurch et al. (2006) and Page et al. (2011), implying that when absorption is found in type 1 AGN it can be modeled in both ways. The above authors also suggested that, between CA and WA, the second is to be preferred since it offers a more physical and testable description of the X-ray data; the WA model also provides a more natural way to explain the variability in the absorption seen in many objects as due to the presence of several distinct ionization phases. A possible location for this ionizing gas could be in an accretion disk wind or in the biconical structure mapped by the [O III] emission line (ionization cones) and seen in some objects, including NGC 4151, MKN 6, NGC 3227 and NGC 3516. The Chandra survey of Extended Emission-line Regions in nearby Seyfert galaxies (CHEERS project) provides some support to the ionization cones hypothesis (Wang et al. 2011, Paggi et al. 2012).

As can be seen in Table 3, for a few cases we do not have detailed information on the nature of absorption, but only

Table 3. Main characteristics of absorbed type 1 Seyferts in INTEGRAL AGN sample

Name	class	N_{HOpt} $\times 10^{22} \text{ cm}^{-2}$	N_{HX} $\times 10^{22} \text{ cm}^{-2}$	type of abs. [†]	instr.	ref for type of abs.
UGC 3142	Sey 1	-	4.0^{+2}_{-1}	CA	XMM	Ricci et al. 2010
IGR J21247+5059	Sey 1	-	$7.9^{+2.02}_{-1.66}$	CA	XMM	Molina et al. 2009
4U 0557-385	Sey 1.2	0.36 ⁽¹⁾	$1.3^{+0.2}_{-0.2}$	WA	XMM	Ashton et al. 2006
IGR J10147-6354	Sey 1.2	-	$2.0^{+1.6}_{-1.1}$	<i>no info</i>	XRT	Rodriguez et al. 2008
MCG-6-30-15	Sey 1.2	0.4-1.1 ⁽²⁾	$1.5^{+0.3}_{-0.4}$	WA	XMM	Molina et al. 2009
IGR J16558-5203	Sey 1.2	-	30^{+11}_{-8}	CA	XMM	Panessa et al. 2008
IGR J19491-1035	Sey 1.2	-	$1.8^{+0.8}_{-0.7}$	<i>no info</i>	XRT	Malizia et al. 2011
QSO B2251-178	Sey 1.2	0.28 ⁽³⁾	$2.1^{+0.6}_{-1.2}$	WA	Suzaku	Winter et al. 2012
Mrk 6	Sey 1.5	0.44 ⁽⁴⁾	$8.12^{+4.76}_{-2.83}$	WA	XMM	Winter et al. 2012
IGR J09253+6929	Sey 1.5	-	14.8^{+28}_{-11}	<i>no info</i>	XRT	Malizia et al. 2011
NGC 3227	Sey 1.5	0.33-0.6 ⁽⁵⁾	$6.7^{+0.4}_{-0.2}$	WA	Suzaku	Markowitz et al. 2009
NGC 3516	Sey 1.5	<0.07 ⁽⁶⁾	$3.2^{+0.4}_{-0.4}$	WA	XMM	Mehdipour et al. 2010
NGC 3783	Sey 1.5	0.18 ⁽⁷⁾	$1.2^{+0.4}_{-0.4}$	WA	Suzaku	Winter et al. 2012
NGC 4151	Sey 1.5	0.13-0.43 ⁽⁸⁾	$21.4^{+13.7}_{-10.4}$	WA	Suzaku	Winter et al. 2012
IGR J12107+3822	Sey 1.5	-	$4.6^{+1.2}_{-1.0}$	<i>no info</i>	XMM	Parisi et al. 2012
4U 1344-60	Sey 1.5	-	$46.8^{+32.4}_{-21.2}$	CA	XMM	Molina et al. 2009
ESO 140-43	Sey 1.5	0.19 ⁽⁹⁾	11^{+3}_{-6}	WA	XMM	Ricci et al. 2010
Swift J1930.5+3414	Sey 1.5	-	$27.5^{+20.4}_{-13.7}$	CA	XRT	Winter et al. 2009
IGR J16185-5928	NLS1	-	$10.6^{+16}_{-5.5}$	CA	XMM	Panessa et al. 2011
IGR J19378-0617	NLS1	0.22-0.64 ⁽¹⁰⁾	$32^{+10.5}_{-8}$	CA	XMM	Panessa et al. 2011

†: CA = complex absorption i.e. multi absorption layers of neutral material; WA = warm absorber i.e. multiple ionized absorbers with different covering factors, column densities and ionization parameters (in both cases we have considered the maximum value of N_H); *no info* = no information on the type of absorption is available. (1) Turner et al. 1996; (2) Pounds et al. 1986; (3) Wu et al. 1980; (4) Feldmeier et al. 1999; (5) Kraemer et al. 2000; (6) Kraemer et al. 2002; (7) Word & Morris 1984; (8) Shapovalova et al. 2010; (9) De Zotti & Gaskell 1985; (10) Mullaney & Ward 2008

a simple neutral column density in excess to the Galactic value. However, for IGR J10147-6354, IGR J19491-1035 and IGR J09253+6929, the N_H estimates are based on rather short (not more than 6 ksec) Swift-XRT observations and so it would be important to have higher quality spectral information before assessing the type of absorption in these sources. We have also re-analysed the Newton-XMM data of IGR J12107+3822 taken from the work of Parisi et al. (2012) which lists a number of objects fitted with a standard basic model. Unfortunately the data are not of high quality, the source remains absorbed in the various models tested, and we cannot exclude at the present stage whether the absorption is simple or rather complex/ionized.

Regarding the possibility that optical/X-ray mismatch is due to variability, we note that a few of the sources listed in Table 3 have changed their classification in time: NGC 4151 from type 1 to type 2 and back, MKN 6 and NGC 3227 from type 2 to type 1 (Osterbrock & Koski 1976, Shapovalova et al. 2009 and Pronik 2009). However, these type of transitions have always been associated to continuum changes with the type 2 designation found when the optical ionizing flux was in a low state. Thus in such objects, the weakness of the broad lines can be entirely independent of obscuration/reddening i.e. these remain type 1 AGN even if temporarily classified as type 2.

In conclusion, we find that no more than 20 objects, corresponding to $13^{+3}_{-2}\%$ of our type 1 sample, have $N_H > 10^{22} \text{ cm}^{-2}$. This percentage has to be considered as an upper

limit; the lower limit can be put at 11% by excluding the 3 sources for which only short XRT exposures are available. This percentage range coincides with that found by Garcet et al. (2007).

We also find that some type 1 AGN in Table 3 have dust-to-gas ratio different than the Galactic one and all have a similar type of absorption. Therefore both explanations put forward to account for absorbed type 1 AGN can work, although the warm ionization hypothesis seems at this stage favoured. In any case, the absorption in these objects seem to be unrelated to the toroidal structure invoked by the AGN unifying theory and so absorbed type 1 sources do not seem to question its validity.

5.2 Unabsorbed type 2 AGN

Ten objects in the sample (see Table 4) are not absorbed in X-rays despite being classified as type 2 AGN. However, 3 of these are of intermediate type and so display evidence for the presence of a broad line region and therefore, following the assumptions we made in section 5, they are expected to be absorbed in X-rays more than type 1, although not as much as type 2 AGN. Indeed the column density distribution for type 1.9 and that for type 2 indicate slightly less absorption in intermediate type objects (see also Risaliti et al. 1999). At least 2 (NGC5995 and IGR J17513-2011) of the 3 Seyfert 1.9 which are unabsorbed in X-rays have a column density close to 10^{22} cm^{-2} . Taking

Table 4. Main characteristics of unabsorbed type 2 Seyferts in INTEGRAL AGN sample

Name	class	N_{HOpt} $\times 10^{22} \text{ cm}^{-2}$	N_{HX} $\times 10^{22} \text{ cm}^{-2}$	type of abs.	instr.	ref
NGC 5995	Sy 1.9	1.18 ⁽¹⁾	0.85 ^{+0.41} _{-0.29}	intr	ASCA	Shu et al 2007
IGR 17513-2011	Sy 1.9	-	0.66 ^{+0.01} _{-0.01}	intr	XMM	De Rosa et al. 2012
IGR J19077-3925	Sy 1.9	0.07 ⁽²⁾	0.14 ^{+0.10} _{-0.08}	intr	XRT	Malizia et al. 2011
IGR J01545+6437	Sy 2	0.25 ⁽²⁾	0.66	Gal	XRT	Malizia et al. 2011
IGR J02504+5443	Sy 2	0.30 ⁽³⁾	0.42	Gal	XRT	Landi et al. 2007
IGR J03249+4041(SW) [†]	Sy 2	1.32 ⁽⁴⁾	>0.15	intr	XRT	Malizia et al. 2011
IGR J07565-4139	Sy 2	>0.9 ⁽⁵⁾	0.72 ^{+0.04} _{-0.04}	intr	XMM	De Rosa et al. 2012
NGC 2992	Sy 2	0.47 ⁽⁶⁾	0.80 ^{+0.05} _{-0.01}	intr	Suzaku	Yaqoob et al. 2007
IGR J14515-5542	Sy 2	-	0.33 ^{+0.17} _{-0.08}	intr	XMM	De Rosa et al. 2012
IGR J16024-6107	Sy 2	0.10 ⁽³⁾	0.25 ^{+0.03} _{-0.01}	intr	XMM	De Rosa et al. 2012

[†] interacting galaxies (see text for details and table in the appendix).

(1) Lumsden et al. 2001; (2) Masetti et al. 2010; (3) Masetti et al. 2008b; (4) Masetti et al. 2012; (5) Masetti et al. 2006; (6) Trippe et al. 2010

into consideration the large uncertainties often associated with the measurement of N_H , these objects can still fit with the unified theory if our line of sight grazes the outer edge of a central obscuring torus. However, this is not the only possible interpretation as intermediate classifications may also be related to other phenomena such as an intrinsically variable ionizing continuum or the presence of absorption/reddening unrelated to the torus: for example a source that would normally appear as a Seyfert 1 can be classified as an intermediate type if it is in a low optical flux state (Trippe et al. 2010) or a source could have the BLR obscured (except for the strongest $H\alpha$ line) by dust related to large scale structures such as bars, dust lanes, and host galaxy plane (Malkan et al. 1998). Unfortunately we do not have sufficient information on these 3 sources to test either hypothesis although we note that NGC 5995 can be classified as an HII galaxy based on some diagnostics and as a Seyfert based on others (Shi et al. 2010), while IGR J19077-3925 is possibly interacting with a nearby object: it is possible that dust unrelated to the torus is present in both AGN in the form of a starburst or due to interaction. The remaining 7 objects are Seyfert 2 not absorbed in X-rays: they make a small fraction (from 6 to 8% allowing for errors on N_H) of all type 2 AGN in the sample. Panessa and Bassani (2002) estimated the percentage of this type of source to be in the range 10%-20%; this number which is derived from a non complete sample, is higher than that found by Risaliti et al. (1999) in a sample of optically selected Seyfert 2 (4%) but consistent with the estimate (12%) made by Caccianiga et al. (2004). Much larger fractions (66-68%) are reported by Page et al. (2006) and Garcet et al. (2007). Despite the above uncertainties, unobscured type 2 AGN may be a non-negligible part of the AGN population and one which mostly questions the AGN unification theory based purely on orientation: they may harbour a genuinely weak or absent broad line region (hence the name of "true" type 2 AGN), and thus are not the simple obscured version of type 1 objects expected from the unified model.

However, before claiming that our 7 sources are true type 2 AGN we should exclude alternative interpretations. For

example it has been argued that some "unobscured" Seyfert 2 galaxies are actually Compton-thick objects in which the direct nuclear component below 10 keV is completely suppressed and we would only witness an unabsorbed spectrum due to scattered nuclear radiation and/or host galaxy emission from a circumnuclear starburst; the presence of heavy obscuration can also be lost in a low S/N X-ray spectrum. A clear signature of the Compton thick nature of a source is the presence of a strong $FeK\alpha$ line with an equivalent width of ~ 1 keV: none of the sources with good quality X-ray data (ASCA, XMM and Suzaku) display such an evidence. On the other hand, XRT spectra do not have sufficient sensitivity to allow the detection of the iron line in weak objects.

Another method to recognize such misclassified Compton thick sources, is to use the diagnostic diagram of Malizia et al. (2007), which plots the X-ray absorption as a function of the source flux ratio $F_{(2-10)keV}/F_{(20-100)keV}$: for our sample of type 2 AGNs this is shown in figure 6 where $\text{Log } N_H$ is the value reported in the table in the Appendix and which is either the intrinsic or the Galactic absorption, this latter being taken again as an upper limit to the X-ray column density. A clear trend of decreasing flux ratios as the absorption increases is expected due to the fact that the 2-10 keV flux is progressively depressed as the absorption becomes stronger. Indeed the two lines shown in the figure describe how the flux ratio changes as a function of N_H in the case of objects characterized by an absorbed power law having a photon index of 1.5 and 1.9 respectively. It is evident that the majority of our sources follow the expected trend with most absorbed AGN showing progressively lower $F_{(2-10)keV}/F_{(20-100)keV}$ values. Misclassified Compton thick AGN are expected to lie in the region of low X-ray flux ratio and low N_H values. Four type 2 AGN: LEDA 96373 (#3), IGR J12288+0052 (#4 a source already discussed in section 4.2), IGR J18311-337 (#5) and IGR J01545+6437 (#6) are located in this region but, while three are absorbed, although not heavily, the only one with N_H below 10^{22} cm^{-2} is IGR J01545+6437.

For this last source the $F_{2-10 \text{ keV}}/F[\text{OIII}]$ ratio² often used as another way to pinpoint heavily absorbed Seyfert 2, is small (0.64) but not so much as to unambiguously classify the source as a Compton thick object (Bassani et al. 1999a). Clearly in this case, where only poor quality X-ray data are available, a statistically more significant X-ray spectrum is needed to better classify this source in terms of absorption. The lack of deep X-ray observations is also the reason that prevents us to give conclusive results in the cases of the other 3 sources (for example the detection of strong iron lines) which, although absorbed, have a low X-ray softness flux ratio; indeed also the $F_{2-10 \text{ keV}}/F[\text{OIII}]$ ratio is not sufficiently constrained to discriminate between Compton thin and Compton thick absorption.

Various other explanations have been proposed to understand the nature of unabsorbed type 2 AGN such as state transitions and non-simultaneous X-ray and optical observations, as already mentioned. Some AGN change their optical classification over time, while others display rapid variations in their X-ray column density: such objects might be classified as unobscured (in X-rays) type 2 objects by chance, if the X-ray and optical data are obtained at different times. One example of such an object is NGC 2992. This source has a long history of variability both in the optical and X-ray regime (Trippe et al. 2008): it was originally classified as a Seyfert 1.9, but it has been seen previously as a Seyfert 1.5 with strong broad $H\alpha$ emission while more recently it changed again to a type 2 AGN. Because the changes in the optical seem to be correlated with the X-ray brightness, it seems that NGC 2992 is a type 1 Seyfert (hence unabsorbed) becoming a type 2 AGN only when the nucleus is in a low continuum state and the broad emission lines are extremely weak or absent. The small absorption present seems to be related to a dust lane in the source rather than to an obscuring torus (Trippe et al. 2008). It is difficult to assess if a similar behaviour is present in other unabsorbed Seyfert 2 galaxies in the sample since we lack a long history of observations for those AGN which have only recently been discovered by INTEGRAL. Nevertheless, for a few objects in Table 4, we find evidence for variability at least in X-rays that could indicate a similarity with NGC 2992. IGR J16024-6107 is seen varying in the INTEGRAL data being a burst source (see Bird et al. 2010 for details) and also between Swift XRT observations (the count rate in the 0.3-10 keV band dropped by a factor of 1.7 over 21 days period).

Also IGR J07565-4139 is seen varying between XRT, Chandra and XMM observations (Malizia et al. 2007, De Rosa et al. 2008, De Rosa et al. 2012) while IGR J14515-5542 shows a different flux when two XMM Slew observations performed 7 months apart are compared.

It is thus important for these objects to perform optical and X-ray spectroscopy as close in time as possible.

Another explanation put forward to interpret unabsorbed type 2 AGN is an extremely high dust-to-gas ratio ($N_{H\text{Opt}}/N_H$) compared with the Galactic value. This option has been poorly explored in the literature because the few

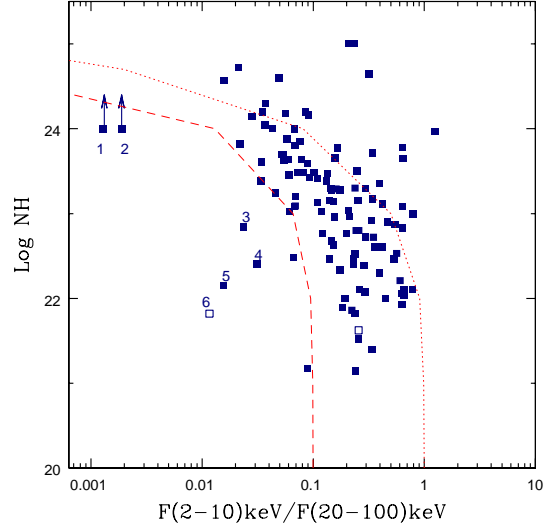


Figure 6. $\text{Log } N_H$ versus $F_{2-10 \text{ keV}}/F_{20-100 \text{ keV}}$ flux ratio of the INTEGRAL type 2 AGN. Open symbols are objects where no intrinsic absorption have been measured and lines correspond to expected values for an absorbed power law with photon index 1.5 (dot) and 1.9 (dash). Sources: #1=IGR J14561-3738, #2=MCG-07-06-018, #3=LEDA 96373, #4=IGR J12288+0052, #5=IGR J18311-337, #6=IGR J01545+6437

measurements so far available indicate that this ratio is generally 3-100 times lower than the Galactic value (Maiolino et al. 2001a). This is basically the reverse situation described in the previous section for absorbed type 1 AGN where observations require more gas than dust; in this case instead we need less absorbing gas and much more optical dust reddening. Also in this case, we have been able to collect E_B-V values intrinsic to the AGN for most of the sources in our sample (see column 3 of Table 4) and have converted them into an optical column density as done in Table 3. In most cases, the optical (dust) absorption is similar within errors to the X-ray (gas) one, implying a dust to gas ratio in the range 0.4-1.4, i.e. similar to the Galactic value, an indication that in these cases this explanation is not appropriate. The only possible exception is IGR J03249+4041(SW), which has an optical reddening of 1.3×10^{22} (Masetti et al. 2012) a factor of 10 higher than the admittedly loose lower limit on the X-ray column density. This suggests that either the X-ray absorption is largely underestimated or that dust is present in large quantities in the source and is responsible for masking the broad line region. IGR J03249+4041(SW) is part of a group of 3 galaxies in a common halo (Lutovinov et al. 2010); at least two galaxies are AGN (IGR J03249+4041(SW) and IGR J03249+4041(NE); see also the table in the Appendix) interacting among themselves, which gives rise to a complex structure (Meusinger et al. 2000). It is therefore not surprising to find such large quantities of dust in this galaxy.

The last possible explanation for unabsorbed type 2 AGN is the dilution effect: broad emission lines in these objects can be overwhelmed by the host galaxy light in addition to being hidden in a low S/N optical spectrum. However, this effect is

² The [OIII] flux is corrected for extinction using the prescription of Bassani et al. (1999a)

unlikely to be important in the spectra acquired within our own optical identification program since their S/N ratio is good enough to characterize the shape of the emission lines. Also the spectral resolution is sensitive enough to definitely assess whether a line is narrow or broad; therefore we do not expect that the contribution of the underlying continuum could alter the classification (Masetti et al. 2012 and references therein).

Finally, it is worth noting that in a few objects of Table 4 the X-ray data are of low statistical significance and of limited spectral coverage (mainly from XRT observations); in these cases it is possible that more refined measurements will provide a more precise estimate of the source column density and a value more in line with the object optical class.

If a source cannot be explained by any of the above hypotheses, then it is probably a "true" type 2 AGN, i.e. a source with a very weak or even absent BLR. After close scrutiny, only a handful of objects have been identified with true unobscured type 2 AGN in the literature (Shi et al. 2010); the main contamination comes from Compton thick AGN not recognized as such for lack of good quality X-ray data or broad band X-ray spectral coverage (Shi et al. 2010) or by type 1 AGN with optical spectra overwhelmed by a luminous host galaxy (Garret et al. 2007). Our set of sources have not been studied in detail to exclude these alternative explanations. Furthermore, although our unabsorbed type 2 AGN tend to be dimmer in X-rays than absorbed ones, their 2–10 (and 20–100) keV luminosities are always above 10^{42} erg s⁻¹: this is incompatible with models (Nicastro 2000; Nicastro et al. 2003; Elitzur & Shlosman 2006) where at low accretion rates (and hence low luminosities) the BLR cannot form.

Therefore we can estimate that at most only half of the sample is still eligible to be classified as a "true" type 2 AGN, i.e. 3–4% of the entire type 2 population, a value similar to the original estimate by Risaliti et al. (1999).

6 SUMMARY AND CONCLUSIONS

In this work we have presented a new INTEGRAL AGN catalogue which, being made by collecting all the AGN from the 4th IBIS catalogue and the Krivonos et al. (2007) IBIS sky survey, represents the most complete view of the INTEGRAL extragalactic sky up to now. It lists 272 AGN for which we have secure optical identifications, precise optical spectroscopy and measured redshift values plus X-ray spectral information, i.e. 2–10 keV and 20–100 keV fluxes and column density.

A list of AGN properly characterized in this way is an ideal tool for population studies.

Here we mainly used this sample to study the absorption properties of active galaxies, to probe new AGN classes and to test the AGN unification scheme; some of the results presented here are the refinement of previous works, while others are obtained here for the first time using a hard X-ray selected sample.

Assuming as a dividing line between absorbed and unabsorbed AGN a column density of 10^{22} cm⁻², we find that half (48%) of the sample is absorbed while the fraction of Compton thick AGN is small ($\sim 7\%$). In line with our previous analysis, we have shown that these fractions suffer from

a bias towards heavily absorbed objects which are lost if weak and at large distance. When this bias is removed, as is possible in the local Universe, the above fractions increase to 80% and 17% (within 60 Mpc) in full agreement with our previous results (Malizia et al. 2009). We also find that absorption is a function of source luminosity, which implies some evolution in the obscuration properties of AGN. Unfortunately it is difficult at the present stage to disentangle between this evolution effect and the bias discussed above as the two are strongly correlated. This important aspect will be explored in the future with a dedicated study.

Among the 272 AGN, a few peculiar classes, so far poorly studied in the hard X-ray band, have been detected for the first time such as 5 XBONG, 5 type 2 QSOs and 11 LINERs. The properties of the 5 XBONG can be explained in terms of heavy obscuration combined with dilution due to a bright galaxy host; given the X-ray luminosity involved, these objects are unlikely to be explained in terms of radiatively inefficient accretion. None of the type 2 QSO is heavily absorbed nor qualifies to be a ERO; type 2 QSO make a small fraction of the sample (2%) and are largely outnumbered by type 1 QSO, suggesting that they are less numerous or more difficult to find. Finally we have been able to observe hard X-ray selected LINERs for the first time: akin to the Seyferts they come in two flavours (type 2 and 1) and, similarly, the first are absorbed while the second are not. All our LINERs are obviously powered by an AGN.

The careful classification of each AGN listed in the catalogue has allowed the study of the correlation between optical classification and X-ray absorption and hence to test the AGN unification model. Although the presence of a correlation is expected and indeed found, i.e. type 1 AGN are typically unabsorbed while type 2 AGN are often absorbed, its strength changes from sample to sample but is never 100%. The outliers are clearly very interesting objects because they question the validity of the Unified Theory and therefore can provide information on how to refine it.

In terms of optical classification, our sample contains 154 objects (57%) which are of type 1 and 118 (43%) which are of type 2; this subdivision is similar to that found in X-rays if unabsorbed versus absorbed objects are considered, suggesting that the match between optical and X-ray classification is good overall. Only a small percentage of sources (12%) does not fulfill the expectation of the Unified Theory as we find 22 type 1 AGN which are absorbed and 10 type 2 AGN which are unabsorbed.

Looking in depth at these sources we conclude that:

- Most of the absorbed type 1 AGN have dust extinction systematically lower than gas absorption, confirming previous results from Maiolino et al. (2001a). More interestingly, however, is the fact that many absorbed type 1 AGN have X-ray spectra characterized by either complex or warm/ionized absorption; these two models provide quite similar fits so that we can conclude that all absorbed type 1 AGN present the same type of absorption, more likely due to ionized gas located in an accretion disk wind or in the biconical structure associated to the central nucleus. Since this type of absorption is unrelated to the toroidal structure invoked by the AGN unifying theory, absorbed type 1 sources do not seem to question its validity.

• We also analysed all 10 type 2 AGN which resulted to be unabsorbed to see if the lack of X-ray absorption could be explained somehow before considering them as "true" type 2 AGN. We found that a) one is possibly a Compton thick object (IGR J01545+6437), b) a few sources are variable in X-rays so that their different optical/X-ray classifications can be explained in terms of state transitions and/or non-simultaneous X-ray and optical observations (NGC 2992, NGC 5995, IGR J16024-6107), c) at least one source could be characterized by an extremely high dust-to-gas ratio (IGR J03249+4041). All together we estimate that at most only half of the sample is still eligible to be classified as a "true" type 2 AGN, i.e. 3-4% of the type 2 sub-sample.

In conclusion, the standard-based AGN unification scheme is followed by the majority (up to 96–97%) of bright AGN, very few outliers are found among type 2 AGN and almost none among type 1 sources; despite absorption being present in a significant fraction of type 1, it is likely unrelated to the torus but rather to ionized gas near the source central engine.

These are some of the results that can be obtained with the present large sample, highlighting the potential of statistical and population studies using hard X-ray selected AGN. Further work involving absorption on a large scale is in progress.

ACKNOWLEDGMENTS

We thank the anonymous referee for her/his valuable comments and suggestions.

This research has made use of data obtained from the SIMBAD database operated at CDS, Strasbourg, France; the High Energy Astrophysics Science Archive Research Center (HEASARC), provided by NASA's Goddard Space Flight Center NASA/IPAC Extragalactic Database (NED). The authors acknowledge the ASI financial support via ASI-INAF grants I/033/10/0 and I/009/10/0.

REFERENCES

- Antonucci, R. 1993, *ARA&A*, 31, 473
 Akylas, A.; Georgantopoulos, I. 2009, *A&A*, 500, 999
 Ashton, C. E.; Page, M. J.; Branduardi-Raymont, G.; Blustin, A. J. 2006, *MNRAS*, 366, 521
 Awaki, H.; Anabuki, N.; Fukazawa, Y.; Gallo, L. C.; Ikeda, S.; et al. 2008, *PASJ*, 60, 293
 Bassani, L.; Cappi, M.; Malaguti, G. 1999b, *ApL&C*, 39, 41
 Bassani, L.; Dadina, M.; Maiolino, R.; Salvati, M.; Risaliti, G. et al. 1999a, *ApJS*, 121, 473
 Bassani, L.; Landi, R.; Malizia, A.; Fiacchi, M. T.; Bazzano, A.; et al. 2007, *ApJ*, 669, 1
 Bassani, L.; Molina, M.; Malizia, A.; Stephen, J. B.; Bird, A. J.; et al. 2006, *ApJ*, 636, 65
 Beckmann, V.; Barthelmy, S. D.; Courvoisier, T. J.-L.; Gehrels, N.; et al. 2007, *A&A*, 475, 827
 Bianchi, S.; Maiolino, R.; Risaliti, G. 2012, *Advances in Astronomy*, vol. 2012, id. 782030
 Bikmaev, I. F.; Burenin, R. A.; Revnivtsev, M. G.; Sazonov, S. Yu.; Sunyaev, R. A.; et al. 2008, *AstL*, 34, 653
 Bird, A. J., Bazzano, A., Bassani, L. et al. 2010, *ApJS*, 186, 1
 Burlon, D.; Ajello, M.; Greiner, J.; Comastri, A.; Merloni, A.; Gehrels, N. 2011, *ApJ*, 728, 58
 Caccianiga, A., Severgnini, P., Braito, V., et al. 2004, *A&A*, 416, 901
 Cappi, M.; Panessa, F.; Bassani, L.; Dadina, M.; Di Cocco, G.; et al. 2006, *A&A*, 446, 459
 Cardelli, J.A., Clayton, G.C., & Mathis, J.S. 1989, *ApJ*, 345, 245
 Churazov, E.; Forman, W.; Jones, C.; Boehringer, H. 2003, *ApJ*, 590, 225
 Civano, F.; Mignoli, M.; Comastri, A.; Vignali, C.; Fiore, F.; et al. 2007, *A&A*, 476, 1223
 Collinge, M. J. and Brandt, W. N. 2000, *MNRAS*, 317, 35
 Comastri, A.; Iwasawa, K.; Gilli, R.; Vignali, C.; Ranalli, P.; et al. 2010, *ApJ*, 717, 787
 Comastri, A.; Mignoli, M.; Ciliegi, P.; Severgnini, P.; Maiolino, R.; et al. 2002, *ApJ*, 571, 771
 Dadina, M. 2007, *A&A*, 461, 1209
 Della Ceca, R.; Caccianiga, A.; Severgnini, P.; Maccacaro, T.; Brunner, H. et al. 2008, *A&A*, 487, 119
 De Rosa, A.; Bassani, L.; Ubertini, P.; Panessa, F.; Malizia, A.; et al. 2008, *A&A*, 483, 749
 De Rosa, A.; Panessa, F.; Bassani, L.; Bazzano, A.; Bird, A. J.; et al. 2012, *MNRAS*, 420, 2087
 De Rosa, A.; Piro, L.; Tramacere, A.; Massaro, E.; Walter, R.; et al. 2005, *A&A*, 438, 121
 De Zotti, G.; Gaskell, C. M. 1985, *A&A*, 147, 1
 Dewangan, G. C.; Griffiths, R. E. 2005, *ApJ*, 625, 31
 Donato, D.; Sambruna, R. M.; Gliozzi, M. 2005, *A&A*, 433, 1163
 Elitzur M., Shlosman I., 2006, *ApJ*, 648, L101
 Elvis, M.; Fiore, F.; Siemiginowska, A.; Bechtold, J.; Mathur, S.; McDowell, J. 2000, *ApJ*, 543, 545
 Eracleous, M.; Hwang, J. A.; Flohic, H. M. L. G 2010, *ApJ Suppl.* 187, 135
 Evans, D. A.; Worrall, D. M.; Hardcastle, M. J.; Kraft, R. P.; Birkinshaw, M. 2006, *ApJ*, 642, 96
 Eguchi, S.; Ueda, Y.; Terashima, Y.; Mushotzky, R.; Tueller, J. 2009, *ApJ*, 699, 1657
 Fabian, A. C.; Iwasawa, K. 1999, *MNRAS*, 303, 34
 Feldmeier, J. J.; Brandt, W. N.; Elvis, M.; Fabian, A. C.; Iwasawa, K.; Mathur, S. 1999, *ApJ*, 510, 167
 Filippenko, A. V.; Ho, L. C. 2003, *ApJ*, 588, 13
 Fiacchi, M.; Bassani, L.; Bazzano, A.; Ubertini, P.; Landi, R.; et al. 2010, *ApJ*, 720, 987
 Gallo, L. C.; Lehmann, I.; Pietsch, W.; Boller, Th.; Brinkmann, W.; et al. 2006, *MNRAS*, 365, 688
 Gandhi, P., Crawford, C. S., Fabian, A. C., et al. 2004, *MNRAS*, 348, 529
 Garcet, O.; Ghandi, P.; Gosset, E.; Sprimont, P.G.; Surdej, J.; et al. 2007, *A&A* 474, 473
 Ghisellini, G.; Foschini, L.; Tavecchio, F.; Pian, E. 2007, *MNRAS*, 382, 82
 Gilli, R.; Comastri, A.; Hasinger, G. 2007, *A&A*, 463, 79
 Grandi, P.; Malaguti, G.; Fiacchi, M. 2006, *ApJ*, 642, 113
 Grandi, P.; Sambruna, R. M.; Maraschi, L.; Matt, G.; Urry, C. M. et al. 1997, *ApJ*, 487, 636
 Greenhill, L. J.; Tilak, A.; Madejski, G. 2008 *ApJ*, 686, 13
 Guainazzi, M.; Fabian, A. C.; Iwasawa, K.; Matt, G.; Fiore, F. 2005a, *MNRAS*, 356, 295
 Guainazzi, M.; Matt, G.; Perola, G. C. 2005b, *A&A*, 444, 119
 Guainazzi, M.; Oosterbroek, T.; Antonelli, L. A.; Matt, G. 2000, *A&A*, 364, 80
 Guainazzi, M.; Rodriguez-Pascual, P.; Fabian, A. C.; Iwasawa, K.; Matt, G. 2004, *MNRAS*, 355, 297
 Hasinger, G.; Miyaji, T.; Schmidt, M. 2005, *A&A*, 441, 417
 Heckman, T. M. 1980, *A&A*, 87, 152
 Ho, L. C. 1999, *AdSpR*, 23, 813
 Ho, L. C.; Filippenko, A. V.; Sargent, W. L. W. 1993, *ApJ*, 417, 63
 Ho, L. C.; Filippenko, A. V.; Sargent, W. L. W. 1997, *ApJS*, 112, 315

- Isobe, N.; Tashiro, M.; Makishima, K.; Iyamoto, N.; Suzuki, M.; et al. 2002, ApJ, 580, 111
- Itoh, T.; Done, C.; Makishima, K.; Madejski, G.; Awaki, H.; et al. 2008, PASJ, 60, 251
- Jimenez-Bailon, E., Guainazzi, M., Matt, G., et al. 2008, RMxAC, 32, 131
- Jimenez-Bailon, E.; Santos-Lleo, M.; Piconcelli, E.; Matt, G.; Guainazzi, M.; Rodriguez-Pascual, P. 2007, A&A, 461, 917
- Kauffmann, G.; Heckman, T. M.; Tremonti, C.; et al. 2003, MNRAS, 346, 1055
- Kraft, R.P.; Hardcastle, M. J.; Worrall, D. M.; Murray, S. S. 2005, ApJ, 622, 149
- Kraemer, S. B.; George, I. M.; Turner, T. J.; Crenshaw, D. M. 2000, ApJ, 535, 53
- Kraemer, S. B.; Crenshaw, D. M.; George, I. M.; Netzer, H.; Turner, T. J.; Gabel, J. R. 2002, ApJ, 577, 98
- Krivonos, R.; Revnivtsev, M.; Lutovinov, A.; Sazonov, S.; Churazov, E.; Sunyaev, R. 2007, A&A, 475, 775
- La Franca, F.; Fiore, F.; Comastri, A.; Perola, G. C.; Sacchi, N.; et al. 2005, ApJ, 635, 864
- Landi, R., Bassani, L., Malaguti, G., Cappi, M., Comastri, A., et al. 2001, A&A, 379, 46
- Landi, R., Bassani, L., Malizia, A., Bazzano, A., Ubertini, P., et al. 2010b, Atel, #2830
- Landi, R.; Bassani, L.; Malizia, A.; Stephen, J. B.; Bazzano, A.; et al. 2010a, MNRAS, 403, 945
- Landi, R.; Malizia, A.; Bazzano, A.; Flocchi, M.; Bird, A. J. et al. 2011, Atel, #2185
- Landi, R.; Malizia, A.; Masetti, N.; de Rosa, A.; Gianni', S.; et al. 2007a, Atel, #1274
- Landi, R.; Malizia, A.; Masetti, N.; De Rosa, A.; Gianni', S.; et al. 2007d, Atel, #1310
- Landi, L., Masetti, N., Bazzano, A., Bird, A.J., Gehrels, N. 2010c, Atel, #3065
- Landi, R.; Masetti, N.; Stephen, J. B.; de Rosa, A.; Capitanio, F.; et al. 2007b, Atel, #1288
- Landi, R.; Masetti, N.; Morelli, L.; Palazzi, E.; Bassani, L.; et al. 2007c, ApJ, 669, 109
- Landi, R., Masetti, N., Bassani, L., Capitanio, F., Flocchi, M.T. et al., 2007d, Atel, #1273
- Longinotti, A. L.; Bianchi, S.; Santos-Lleo, M.; Rodriguez-Pascual, P.; Guainazzi, M. et al. 2007, A&A, 470, 73
- Lumsden, S.L.; Heisler, C.A.; Bailey, J.A.; Hough, J.H.; Young, S. 2001, MNRAS, 327, 459
- Lutovinov, A.; Burenin, R.; Sazonov, S.; et al. 2010, ATel, #2759
- Maiolino, R., Marconi, A., Salvati, M., et al. 2001a, A&A, 365, 28
- Maiolino, R., Marconi, A., Oliva, E. 2001b, A&A, 365, 37
- Mainieri, V.; Bergeron, J.; Hasinger, G.; Lehmann, I.; Rosati, P.; et al. 2002, A&A, 393, 425
- Maiorano, E.; Landi, R.; Stephen, J. B.; Bassani, L.; Masetti, N.; et al. 2011, MNRAS, 416, 531
- Malizia, A.; Bassani, L.; Landi, R.; Bazzano, A.; Bird, A. J.; Panessa, F. 2011, Proceedings of Science, SISSA, conf. ID 147
- Malizia, A.; Bassani, L.; Panessa, F.; De Rosa, A.; Bird, A. J. 2009, MNRAS, 394, 121
- Malizia, A.; Landi, R.; Bassani, L.; Bird, A. J.; Molina, M. et al. 2007, ApJ, 668, 81
- Malkan, M. A.; Gorjian, V.; Tam, R. 1998, ApJS, 117, 25
- Markowitz, A.; Takahashi, T.; Watanabe, S.; Nakazawa, K.; Fukazawa, Y. et al. 2007, ApJ, 665, 259
- Matsumoto, C.; Nava, A.; Maddox, L. A.; Leighly, K. M.; Grupe, D.; et al. 2004, ApJ, 617, 930
- Matt, G.; Bianchi, S.; Guainazzi, M.; Molendi, S. 2004, A&A, 414, 155
- Masetti, N.; Mason, E.; Landi, R.; Giommi, P.; Bassani, L.; et al. 2008a, A&A, 480, 715
- Masetti, N.; Mason, E.; Morelli, L.; Cellone, S.A.; McBride, V.A.; et al. 2008b, A&A, 482, 113
- Masetti, N.; Morelli, L.; Palazzi, E.; Galaz, G.; Bassani, L.; et al. 2006, A&A, 259, 21
- Masetti, N.; Parisi, P.; Jimenez-Bailon, E.; Palazzi, E.; Chavushyan, V.; et al. 2012, A&A, 538, 123
- Masetti, N.; Parisi, P.; Palazzi, E.; Jimenez-Bailon, E.; Chavushyan, V.; et al. 2010, A&A, 519, 96
- Massaro, F.; Harris, D. E.; Tremblay, G. R.; Axon, D.; Baum, S. A.; et al. 2010, ApJ, 714, 589
- Mateos, S., Carrera, F. J., Page, M. J., Watson, M. G., Corral, A. et al. 2010, A&A, 510, 35
- Mehdipour, M.; Branduardi-Raymont, G.; Page, M. J. 2010, MNRAS, 514, 100
- Meusinger, H.; Brunzendorf, J.; Krieg, R. 2000, A&A, 363, 933
- Miniutti, G.; Ponti, G.; Dadina, M.; Cappi, M.; Malaguti, G. et al. 2006, MNRAS, 373, L1
- Molina, M.; Bassani, L.; Malizia, A.; Bird, A. J.; Dean, A. J.; et al. 2008, MNRAS, 390, 1217
- Molina, M.; Bassani, L.; Malizia, A.; Stephen, J. B.; Bird, A. J.; et al. 2009, MNRAS, 399, 1293
- Moran, E. C., Filippenko, A. V., Chornock, R. 2002, ApJ, 579, 71
- Mullaney, J. R.; Ward, M.J., 2008, MNRAS, 385, 53
- Murray, N., Chiang, J., Grossman, S. A., et al. 1995, ApJ, 451, 498
- Nicastro F., 2000, ApJ, 530, L65
- Nicastro F., Martocchia A., Matt G., 2003, ApJ, 589, L13
- Noguchi, K.; Terashima, Y.; Awaki, H. 2009, ApJ, 705, 454
- Osterbrock, D. E.; Koski, A. T. 1976, MNRAS, 176, 61
- Page, M. J., Carrera, F. J., Stevens, J. A., Ebrero, J., Blustin, A. J. 2011, MNRAS, 416, 2792
- Page, M. J., Loaring, N. S., Dwelly, T., et al. 2006, MNRAS, 369, 156
- Paggi, A.; Wang, J.; Fabbiano, G.; Elvis, M.; Karovska, M. 2012, arXiv:1203.1279
- Panessa, F.; Bassani, L. 2002, A&A, 394, 435
- Panessa, F.; Bassani, L.; De Rosa, A.; Bird, A. J.; Dean, A. J.; et al. 2008, A&A, 483, 151
- Panessa, F.; De Rosa, A.; Bassani, L.; Bazzano, A.; Bird, A.; et al. 2011, MNRAS, 417, 2426
- Papadakis, I. E.; Ioannou, Z.; Brinkmann, W.; Xilouris, E. M. 2008, A&A, 490, 995
- Parisi, P.: et al. 2012, *in preparation*
- Piconcelli, E.; Bianchi, S.; Guainazzi, M.; Fiore, F.; Chiaberge, M. 2007, A&A, 466, 855
- Piconcelli, E., Jimenez-Bailon, M., Guainazzi, M., Scharrel N., Rodriguez-Pascual, P.M. et al. 2005, A&A, 432, 15
- Pounds, K. A.; Turner, T. J.; Warwick, R. S. 1986, MNRAS, 221, 7
- Pronik, I. I. 2009, A&A, 496, 299
- Reeves, J. N.; Awaki, H.; Dewangan, G. C.; Fabian, A. C.; Fukazawa, Y.; et al. 2007 PASJ, 59, 301
- Revnivtsev, M.; Sunyaev, R.; Lutovinov, A.; Sazonov, S. 2007, Atel, #1253
- Ricci, C.; Beckmann, V.; Audard, M.; Courvoisier, T. J.-L. 2010, A&A, 518, 47
- Risaliti, G.; Elvis, M.; Nicastro, F. 2002, ApJ, 571, 234
- Risaliti, G.; Maiolino, R.; Salvati, M. 1999, ApJ, 522, 157
- Risaliti, G.; Salvati, M.; Elvis, M.; Fabbiano, G.; Baldi, A.; et al. 2009, MNRAS, 393, 1
- Rodriguez, J.; Tomsick, J. A.; Bodaghee, A. 2010, A&A, 517, 14
- Rodriguez, J.; Tomsick, J. A.; Chaty, S. 2008, A&A, 482, 731
- Rodriguez, J.; Tomsick, J. A.; Chaty, S. 2009, A&A, 494, 417
- Sazonov, S.; Churazov, E.; Revnivtsev, M.; Vikhlinin, A.; Sunyaev, R. 2005, A&A, 444, 37
- Sazonov, S.; Revnivtsev, M.; Burenin, R.; Churazov, E.; Sunyaev, R.; et al. 2008, A&A, 487, 509

- Sazonov, S.; Revnivtsev, M.; Krivonos, R.; Churazov, E.; Sunyaev, R. 2007, *A&A*, 462, 57
- Scott, A. E., Stewart, G. C., Mateos, S.; Alexander, D. M. et al. 2011, *MNRAS*, 417, 992
- Severgnini, P.; Caccianiga, A.; Della Ceca, R.; Moretti, A.; Vignali, C.; et al. 2011, *A&A*, 525, 38
- Severgnini, P.; Della Ceca, R.; Braito, V.; Saracco, P.; Longhetti, M.; et al. 2005, *A&A*, 431, 87
- Schurch, N. J.; Griffiths, R. E.; Warwick, R. S. 2006, *MNRAS*, 371, 211
- Shapovalova, A. I.; Popovic, L. C.; Bochkarev, N. G.; Burenkov, A. N.; Chavushyan, V. H. et al. 2009, *NewAR*, 53, 193
- Shapovalova, A. I.; Popovic, L. C.; Burenkov, A. N.; Chavushyan, V. H.; Ilic, D.; et al. 2010, *A&A*, 509, 106
- Shi, Y.; Rieke, G. H.; Smith, P.; Rigby, J.; Hines, D.; et al. 2010, *ApJ*, 714, 115
- Shinozaki, K.; Miyaji, T.; Ishisaki, Y.; Ueda, Y.; Ogasaka, Y. 2006, *AJ*, 131, 2843
- Shu, X. W.; Wang, J. X.; Jiang, P.; Fan, L. L.; Wang, T. G. 2007, *ApJ*, 657, 167
- Silverman J. D., Green P. J., Barkhouse W. A., et al. 2005, *ApJ*, 618, 123
- Tomsick, J. A.; Chaty, S.; Rodriguez, J.; Walter, R. 2007, *Atel*, #1018
- Tozzi, P.; Gilli, R.; Mainieri, V.; Norman, C.; Risaliti, G.; et al. 2006, *A&A*, 451, 457
- Trippe, M. L.; Crenshaw, D. M.; Deo, R. P.; Dietrich, M.; Kraemer, S. B. 2008, *AJ*, 135, 2048
- Trippe, M. L.; Crenshaw, D. M.; Deo, R. P.; Dietrich, M.; Kraemer, S. B.; et al. 2010, *ApJ*, 725, 1749
- Trump, J. R.; Impey, C. D.; Taniguchi, Y.; Brusa, M.; Civano, F.; et al. 2009, *ApJ*, 706, 797
- Turner, T. J.; Miller, L.; George, I. M.; Reeves, J. N. 2006, *A&A*, 445, 59
- Turner, T. J.; Netzer, H.; George, I. M. 1996, *ApJ*, 463, 134
- Ueda, Y., Akiyama, M.; Ohta, K.; Miyaji, T. 2003, *ApJ*, 598, 886
- Ueda, Y.; Eguchi, S.; Terashima, Y.; Mushotzky, R.; Tueller, J. et al. 2007, *ApJ*, 664L, 79
- Veron-Cetty, M.-P.; Veron, P. 2010, *A&A*, 518, 10
- Veilleux, S., & Osterbrock, D. E. 1987, *ApJS*, 63, 295
- Vignali, C., Alexander, D. M., Gilli, R., Pozzi, F. 2010, *MNRAS*, 404, 48
- Vignali, C.; Comastri, A. 2002, *A&A*, 381, 834
- Vignati, P.; Molendi, S.; Matt, G.; Guainazzi, M.; Antonelli, A., et al. 1999, *A&A*, 349, 57
- Weingartner, J. C., & Murray, N. 2002, *ApJ*, 580, 88
- Winkler, H. 1992, *MNRAS*, 257, 677
- Winter, L. M.; Mushotzky, R. 2010, *ApJ*, 719, 737
- Winter, L. M.; Mushotzky, R. F.; Reynolds, C. S.; Tueller, J. 2009, *ApJ*, 690, 1322
- Winter, L. M.; Mushotzky, R. F.; Tueller, J.; Markwardt, C. 2008, *ApJ*, 674, 686
- Winter, L. M.; Veilleux, S.; McKernan, B.; Kallman, T. R. 2012, *ApJ*, 745, 107
- Wang, J.; Fabbiano, G.; Elvis, M.; Risaliti, G.; Karovska, M.; et al. 2011, *ApJ*, 742, 23
- Ward, M.; Morris, S. 1984, *MNRAS*, 217, 867
- Wu, C.-C.; Boggess, A.; Gull, T. R. 1980, *ApJ*, 242, 14
- Yamada, S.; Itoh, T.; Makishima, K.; Nakazawa, K. 2009, *PASJ*, 61, 309
- Yaqoob, T.; Murphy, K. D.; Griffiths, R. E.; Haba, Y.; Inoue, H.; et al. 2007, *PASJ*, 59, 283
- Young, A. J.; Wilson, A. S.; Terashima, Y.; Arnaud, K. A.; Smith, D. A. 2002, *ApJ*, 564, 176
- Zhang, S.; Chen, Y.; Collmar, W.; Foschini, L.; Li, T.; et al. 2008, *ApJ*, 683, 400
- Zombeck, M. V. *Book-Review - Handbook of Space Astronomy and Astrophysics* 1990, Science, Vol. 249, NO. 4974

APPENDIX A: INTEGRAL/IBIS AGN SAMPLE

In this Appendix we report the table containing the optical coordinate, redshift, class, 20-100 keV flux and X-ray data (2-10 keV flux, column density and reference work from which these data) for the full AGN sample presented and discussed in this work.

NOTES on table A1: Names in bold are for hard X-ray sources from the INTEGRAL all-sky survey by Krivonos et al. 2007 (see text).

$F_H^\dagger = F_{20-100 \text{ keV}}$ in units of $10^{-11} \text{ erg cm}^{-2} \text{ s}^{-1}$

$F_S^{\dagger\dagger} = F_{2-10 \text{ keV}}$ in units of $10^{-11} \text{ erg cm}^{-2} \text{ s}^{-1}$

◇ value of N_H in bold are Galactic column density measured in the source direction (see text)

* flux variability

(a) interacting galaxies where the INTEGRAL/IBIS detection is referred to both galaxies and the 20-100 keV flux has been estimated to be 50% to each galaxy (see text for details).

(b) this source has a wrong name (ESO 548-G01) in the 4th IBIS catalogue, here the right name and the right redshift has been reported

(c) a different value of column density comes from a published Chandra observation (Tomsick et al. 2007) where it is not clear whether the authors include Galactic absorption or not in their estimate of N_H . This source has now been observed by XRT and these more recent data provide a column density of $N_H = 0.95_{-0.30}^{+0.34} \times 10^{22} \text{ cm}^{-2}$; since the Galactic absorption in the source direction is $\sim 10^{22} \text{ cm}^{-2}$ it is very likely that the Chandra estimate includes both Galactic and intrinsic absorption.

(d) INTEGRAL flux comes from the whole map and has to be considered as a lower limit since the source has been best detected in a revolution map likely during a flare. Its variability and its black hole mass (Masetti et al. 2010) are typical of hard X-ray selected blazars, however the lack of radio detection poses still some doubts on the blazar nature.

(e) ESO 138-1 and NGC 6221 are blended in the IBIS maps and through a simulation we have estimated the contribution of each source in the 20-100 keV band which is almost 50%

(f) for this source we have very recently obtained XMM data. The preliminary analysis indicates that the column density is $0.81_{-0.04}^{+0.05} \times 10^{22} \text{ cm}^{-2}$; this value is compatible with that measured by XRT (Molina et al 2009) but the uncertainty is now sufficiently small to consider the source as not absorbed.

(g) pair of galaxies MCG+04-48-002 (#1) and NGC 6921 (#2) where the INTEGRAL/IBIS detection is referred to both galaxies and the 20-100 keV flux of each has been estimated.

Table A1: INTEGRAL/IBIS AGN

Name	RA	Dec	z	Class	F_H^\dagger	F_S^{\ddagger}	$\text{Log } N_H^\circ$	Reference
IGR J00040+7020	00 04 01.92	+70 19 18.5	0.096	Sy2	1.47	0.35	22.52 [22.49 – 22.54]	De Rosa et al. 2012
IGR J00158+5605	00 15 54.19	+56 02 57.5	0.169	Sy1.5	<0.66	0.31	21.50	Malizia et al. 2011
IGR J00256+6821	00 25 32.50	+68 21 44.0	0.012	Sy2	1.47	0.05	23.60 [22.92 – 23.93]	Landi et al. 2007a
IGR J00333+6122	00 33 18.34	+61 27 43.3	0.105	Sy1.5	1.38	0.68	21.93 [21.65 – 22.11]	Molina et al. 2009
1ES 0033+595	00 35 52.60	+59 50 05.0	0.086	BL Lac	1.83	5.90	21.55 [21.44 – 21.64]	Donato et al. 2005
IGR J00465-4005	00 46 20.68	-40 05 49.1	0.201	Sy2	3.56	0.12	23.38 [23.25 – 23.52]	Landi et al. 2010a
MKN 348	00 48 47.10	+31 57 25.0	0.015	Sy2	10.60	0.44	23.02 [22.93 – 23.10]	Tartarus Database
NGC 526A	01 23 54.40	-35 03 56.0	0.019	Sy1.9	5.34	1.80	22.23 [22.19 – 22.28]	Landi et al. 2001
RX J0137.7+5814	01 37 50.49	+58 14 11.0	-	BL Lac	<0.68	1.01	21.60	Malizia et al. 2011
ESO 297-18	01 38 37.10	-40 00 41.0	0.025	Sy2	6.08	0.33	23.66 [23.62 – 23.70]	Ueda et al. 2007
IGR J01528-0326	01 52 49.00	-03 26 48.5	0.017	Sy2	2.60	0.40	23.15 [23.14 – 23.29]	Landi et al. 2007a
IGR J01545+6437	01 54 35.29	+64 37 57.5	0.034	Sy2	<0.83	0.0097	< 21.82	Malizia et al. 2011
NGC 788	02 01 06.40	-06 48 56.0	0.0136	Sy2	6.00	0.61	23.48 [23.43 – 23.56]	De Rosa et al. 2012
Mrk 1018	02 06 16.00	-00 17 29.0	0.0424	Sy1	1.70	1.19	20.41	Winter et al. 2009
IGR J02086-1742	02 08 34.95	-17 39 34.8	0.129	Sy1.2	2.75	0.64	<20.23	Rodriguez et al. 2010
IGR J02097+5222	02 09 34.30	+52 22 48.0	0.0492	Sy1	2.81	1.30	21.23	Malizia et al. 2007
Mrk 590	02 14 33.50	-00 46 00.0	0.02638	Sy1	1.46	0.64	20.42	Longinotti et al. 2007
SWIFT J0216.3+5128	02 16 26.73	+51 25 25.1	0.422	Sy2 ?	1.62	1.27	22.10 [22.05 – 22.15]	Malizia et al. 2007
SWIFT J0218.0+7348	02 17 30.83	+73 49 32.5	2.367	QSO/Blazar	2.70	0.55	21.54 [21.17 – 21.75]	Winter et al. 2009
Mrk 1040	02 28 14.50	+31 18 42.0	0.0166	Sy1.5	5.19	0.51	20.56 [21.45 – 21.64]	Winter et al. 2009
IGR J02343+3229	02 34 20.10	+32 30 20.0	0.0162	Sy2, LINER	4.74	0.82	22.34 [22.25 – 22.41]	Rodriguez et al. 2008
NGC 985	02 34 37.80	-08 47 15.0	0.043	Sy1.5	2.38	5.40	20.50	Winter et al. 2009
NGC 1052	02 41 04.80	-08 15 21.0	0.005	Sy2, LINER	1.69	0.40	23.30 [23.18 – 23.36]	Guainazzi et al. 2000
RBS 345	02 42 14.60	+05 30 36.0	0.069	Sy1	2.02	0.26	20.72	Malizia et al. 2011
NGC 1068	02 42 40.70	-00 00 48.0	0.0038	Sy2	2.36	0.50	>25.00	Matt et al. 2004
QSO B0241+62	02 44 57.69	+62 28 06.5	0.044	Sy1.2	5.17	3.6	21.32 [21.04 – 21.56]	Molina et al. 2009
MCG -07-06-018	02 46 37.00	-42 22 01.0	0.0696	XBONG	3.72	0.007	>24	Sazonov et al. 2008
IGR J02504+5443	02 50 42.59	+54 42 17.7	0.015	Sy2	1.87	0.48	< 21.62	Landi et al. 2007a
MCG -02-08-014	02 52 23.40	-08 30 37.0	0.0167	Sy2 ?	1.88	1.20	23.08 [22.95 – 23.18]	Rodriguez et al. 2010
NGC 1142	02 55 12.20	-00 11 01.0	0.0288	Sy2	6.12	0.42	23.80 [23.79 – 23.81]	De Rosa et al. 2012
NGC 1194	03 03 49.10	-01 06 13.0	0.0136	Sy2	2.57	0.09	24.20 [23.91 – 24.15]	Greenhill et al. 2008
B3 B0309+411B	03 13 01.96	+41 20 01.2	0.136	Sy1	<2.49	2.36	21.11	Molina et al. 2008
SWIFT J0318.7+6828	03 18 19.02	+68 29 32.1	0.0901	Sy1.9	<0.91	0.73	22.61 [22.57 – 22.66]	Winter et al. 2008
NGC 1275	03 19 48.16	+41 30 42.1	0.0175	Sy1.5/LINER	3.82	1.23	21.08 [21.04 – 21.11]	Churazov et al. 2003
1H 0323+342	03 24 41.16	+34 10 45.8	0.061	NLS1	3.96	0.64	21.16	Panessa et al. 2011
IGR J03249+4041-SW^(a)	03 25 13.20	+40 41 55.0	0.0477	Sy2	1.35	0.12	>21.18	Malizia et al. 2011
IGR J03249+4041-NE^(a)	03 25 12.20	+40 42 02.0	0.0475	Sy2	1.35	0.09	22.48 [22.31 – 22.66]	Malizia et al. 2011
IGR J03334+3718	03 33 18.79	+37 18 11.1	0.05583	Sy1.5	2.61	0.61	21.15 [20.90 – 21.30]	Malizia et al. 2011
NGC 1365	03 33 36.31	-36 08 27.8	0.0054	Sy1.9	4.10	1.30	24.65 [24.58 – 24.78]	Risaliti et al. 2009
NRAO 140	03 36 30.10	+32 18 29.0	1.2580	QSO/Blazar	2.46	0.72	21.10	Donato et al. 2005
ESO 548-G81 ^(b)	03 42 03.7	-21 14 40.0	0.0145	Sy1	4.45	1.35	20.36	Winter et al. 2008
IGR J03532-6829	03 52 57.00	-68 31 18.0	0.087	BL Lac	<8.52	1.75	20.95 [20.70 – 21.11]	Rodriguez et al. 2008
3C 098	03 58 55.00	+10 26 24.0	0.0304	Sy2	3.96	0.27	23.08 [23.00 – 23.18]	Evans et al. 2006

Name	RA	Dec	z	Class	F_H^\dagger	F_S^\dagger	$\text{Log } N_H^\circ$	Reference
4C03.8	04 07 16.45	+03 42 25.9	0.089	Sy2	3.45	0.21	23.45 [23.40 – 23.47]	Winter et al. 2009
3C 111	04 18 21.28	+38 01 35.8	0.0485	Sy1	10.40	3.51	21.66 [21.63 – 21.69]	Molina et al. 2009
IGR J04221+4856	04 22 00.50	+48 56 04.0	0.114	Sy1	1.42	0.37	21.85	this work
LEDA 15023	04 23 40.80	+04 08 03.0	0.045	Sy2	1.87	0.13	23.48 [23.32 – 23.59]	Malizia et al. 2011
3C120	04 33 11.09	+05 21 15.6	0.033	Sy1.5	7.98	4.60	21.20 [21.19 – 21.22]	Grandi et al. 1997
UGC 3142	04 43 46.89	+28 58 19.0	0.0216	Sy1	4.87	1.70	22.60 [22.48 – 22.78]	Ricci et al. 2010
LEDA 168563	04 52 04.79	+49 32 44.6	0.029	Sy1	5.55	4.52	21.73	Molina et al. 2009
SWIFT J0453.4+0404	04 53 25.74	+04 03 41.6	0.0296	Sy2	2.19	0.20	24.16 [24.18 – 24.11]	Severgnini et al. 2011
ESO 033-G02	04 55 59.05	–75 32 28.3	0.0181	Sy2	2.42	1.59	22.10 [21.92 – 22.28]	Risaliti et al. 2002
LEDA 075258	05 02 09.00	+03 31 50.0	0.01599	Sy1	1.26	0.55	19.75 [19.74 – 19.77]	Malizia et al. 2011
SWIFT J0505.8-2348	05 05 45.70	–23 51 14.0	0.03504	Sy2	5.49	1.36	23.50 [23.36 – 23.55]	Eguchi et al. 2009
4U 0517+17	05 10 45.50	+16 29 55.0	0.0179	Sy1.5	6.83	2.53	20.95 [20.90 – 21.04]	Molina et al. 2009
Ark 120	05 16 11.48	–00 09 00.6	0.0327	Sy1	6.55	2.87	20.99	Winter et al. 2009
SWIFT J0519.5-3140	05 19 35.81	–32 39 28.0	0.0126	Sy1.5	4.34	0.34	21.90 [21.60 – 22.04]	Winter et al. 2012
PICTOR A	05 19 49.69	–45 46 44.5	0.0351	Sy1, LINER	<3.36	1.13	20.78	Winter et al. 2009
PKS 0521-36	05 22 58.00	–36 27 31.0	0.0565	Sy1	2.19	1.10	20.55	Winter et al. 2009
PKS 0528+134	05 30 56.42	+13 31 54.9	2.060	QSO/Blazar	1.50	2.57*	21.38	Donato et al. 2005
QSO J0539-2839	05 39 54.3	–28 39 56.0	3.1040	QSO/Blazar	1.74	0.17	21.20	Winter et al. 2009
NGC 2110	05 52 11.38	–07 27 22.4	0.0078	Sy2	17.90	2.50	22.46 [22.59 – 22.63]	Bassani et al. 1999b
MCG+08-11-011	05 54 53.63	+46 26 21.8	0.0205	Sy1.5	8.46	5.62	21.32	Molina et al. 2009
4U 0557-385	05 58 02.05	–38 20 04.6	0.0339	Sy1.2	<2.76	2.00	22.11 [22.04 – 22.18]	Ashton et al. 2006
IRAS 05589+2828	06 02 09.70	+28 28 17.0	0.033	Sy1	4.02	1.64	21.66	Winter et al. 2009
SWIFT J0601.9-8636	06 05 39.60	–86 37 54.0	0.0064	Sy2	2.59	0.11	24.00 [23.80 – 24.19]	Ueda et al. 2007
IGR J06058-2755	06 05 48.96	–27 54 40.1	0.0900	Sy1.5	1.98	0.66	20.38	Malizia et al. 2011
Mrk 3	06 15 36.31	+71 02 14.9	0.0135	Sy2	9.53	0.65	24.00 [23.97 – 24.02]	Awaki et al. 2008
IGR J06233-6436	06 23 07.70	–64 36 20.0	0.12889	Sy1	1.56	0.46	20.59	Gallo et al. 2006
IGR J06239-6052	06 23 45.61	–60 58 45.4	0.0405	Sy2	<0.98	0.32	23.35 [23.44 – 23.63]	Revnivtsev et al. 2007
SWIFT J0640.4-2554	06 40 11.69	–25 53 43.4	0.0248	Sy1.2	3.83	1.88	21.38 [21.36 – 21.40]	Winter et al. 2008
IGR J06415+3251	06 41 23.00	+32 55 39.0	0.01719	Sy2	4.74	0.33	23.20 [23.14 – 23.27]	Winter et al. 2008
Mrk 6	06 52 12.36	+74 25 37.2	0.0188	Sy1.5	4.32	2.51	22.90 [22.72 – 23.11]	Molina et al. 2009
IGR J06523+5334	06 52 31.41	+53 34 31.5	0.301	Sy1.2/QSO	<4.83	0.02	20.81	Landi et al. 2011
LEDA 96373	07 26 26.30	–35 54 21.0	0.0294	Sy2	2.25	0.05	22.84 [22.50 – 23.23]	Landi et al. 2010a
IGR J07565-4139	07 56 19.62	–41 37 42.1	0.021	Sy2	1.43	0.32	21.86 [21.80 – 21.88]	De Rosa et al. 2012
IGR J07597-3842	07 59 41.82	–38 43 56.0	0.04	Sy1.2	3.51	2.37	21.78	Molina et al. 2009
ESO 209-12	08 01 57.60	–49 46 42.0	0.0405	Sy1.5	2.25	8.30	21.38	Panessa et al. 2008
PG0804+761	08 10 58.65	+76 02 42.5	0.1	Sy1	<1.53	1.00	20.70 [20.56 – 20.80]	Shinozaki et al. 2006
IGR J08190-3835	08 19 11.36	–38 33 10.5	0.009	Sy2	1.36	0.15	23.13 [22.84 – 23.41]	Maiorano et al. 2011
FRL 1146	08 38 30.70	–35 59 35.0	0.0316	Sy1.5	2.10	1.26	21.45 [21.30 – 21.54]	Molina et al. 2009
QSO B0836+710	08 41 24.36	+70 53 42.1	2.172	QSO/Blazar	5.77	2.63	20.47	Donato et al. 2005
IGR J08557+6420	08 55 12.54	+64 23 45.5	0.037	Sy2 ?	1.74	0.28	23.29 [23.19 – 23.38]	Malizia et al. 2011
IGR J08558+0814	08 55 58.60	+08 13 19.0	0.22	Sy1	<3.49	0.0065	20.67	Malizia et al. 2011
IGR J09025-6814	09 02 39.46	–68 13 36.6	0.014	XBONG	1.96	0.92	22.90 [22.30 – 24.12]	Rodriguez et al. 2009

Name	RA	Dec	z	Class	F_H^\dagger	F_S^\dagger	$\text{Log } N_H^\circ$	Reference
IGR J09026-4812 ^(c)	09 02 37.31	-48 13 33.9	0.0391	Sy1	2.42	0.46	21.98 [21.81 – 22.11]	this work
SWIFT J0917.2-6221	09 16 09.41	-62 19 29.5	0.0573	Sy1	1.91	1.43	21.61 [21.43 – 21.73]	Molina et al. 2009
MCG-01-24-012	09 20 46.31	-08 03 21.9	0.0196	Sy2	4.06	1.00	22.80 [22.76 – 22.83]	Shinozaki et al. 2006
Mrk 110	09 25 12.85	+52 17 10.5	0.0353	NLS1	5.06	2.79	20.30 [20.00 – 20.48]	Winter et al. 2009
IGR J09253+6929	09 25 47.56	+69 27 53.6	0.039	Sy1.5	<1.94	0.05	23.15 [22.58 – 23.63]	Malizia et al. 2011
IGR J09446-2636	09 44 37.02	-26 33 55.4	0.1425	Sy1.5	<2.34	0.5	20.81	Malizia et al. 2011
NGC 2992	09 45 42.05	-14 19 35.0	0.0077	Sy2	6.51	1.20*	21.90 [21.88 – 21.92]	Yaqoob et al. 2007
NGC-05-23-016	09 47 40.17	-30 56 55.9	0.0085	Sy2	14.50	8.76	22.21 [22.20 – 22.22]	Reeves et al. 2007
IGR J09523-6231	09 52 20.70	-62 32 37.0	0.252	Sy1.9	1.43	0.37	22.80 [22.77 – 22.83]	De Rosa et al. 2012
NGC 3081	09 59 29.54	-22 49 34.6	0.0079	Sy2	5.91	0.13	23.82 [23.70 – 23.92]	Shu et al. 2007
SWIFT J1009.3-4250	10 09 48.22	-42 48 40.4	0.033	Sy2	2.81	0.31	23.41 [23.38 – 23.43]	De Rosa et al. 2012
IGR J10147-6354	10 14 15.55	-63 51 50.1	0.202	Sy1.2	<1.07	0.21	22.30 [21.95 – 22.56]	Rodriguez et al. 2008
NGC 3227	10 23 30.61	+19 51 53.8	0.0038	Sy1.5	11.30	0.81	22.83 [22.81 – 22.85]	Cappi et al. 2006
NGC 3281	10 31 52.06	-34 51 13.3	0.0107	Sy2	5.11	0.29	24.18 [24.11 – 24.23]	Vignali et al. 2002
SWIFT J1038.8-4942	10 38 45.20	-49 46 53.2	0.06	Sy1.5	2.00	1.45	21.79 [21.72 – 21.87]	Malizia et al. 2007
IGR J10404-4625	10 40 22.55	-46 25 25.7	0.024	Sy2	3.36	1.20	22.61 [22.60 – 22.62]	De Rosa et al. 2012
MCG+04-26-006	10 46 42.67	+25 55 52.5	0.02	LINER	3.19	0.22	23.09 [22.93 – 23.23]	Landi et al. 2010a
Mrk 421	11 04 27.31	+38 12 31.8	0.0300	BL Lac	37.65	47.9*	20.89 [20.84 – 20.92]	Donato et al. 2005
NGC 3516	11 06 47.50	+72 34 07.0	0.0088	Sy1.5	5.55	2.3*	22.50 [22.45 – 22.56]	Mehdipour et al. 2010
IGR J11366-6002	11 36 42.04	-60 03 06.6	0.014	Sy2, LINER	1.02	0.46	22.40 [22.02 – 22.61]	Landi et al. 2007b
NGC 3783	11 39 01.78	-37 44 18.7	0.0097	Sy1.5	13.30	6.03	22.06 [21.89 – 22.18]	Molina et al. 2009
H1143-182	11 45 40.47	-18 27 15.5	0.0329	Sy1.5	<4.89	1.43	20.48	Winter et al. 2009
PKS 1143-696	11 45 53.62	-69 54 01.8	0.244	Sy1.2	1.36	0.54	21.21	Landi et al. 2010a
SWIFT J1200.8+0650	12 00 57.92	+06 48 23.1	0.0360	Sy2	1.72	0.58	22.92 [22.68 – 22.94]	Landi et al. 2007c
IGR J12026-5349	12 02 47.63	-53 50 07.7	0.028	Sy2	3.72	0.85	22.41 [22.43 – 22.49]	De Rosa et al. 2012
NGC 4051	12 03 09.62	+44 31 52.8	0.0023	NLS1	3.59	0.63	<21.48	Cappi et al. 2006
NGC 4074	12 04 29.65	+20 18 58.2	0.0224	Sy2	2.19	0.18	23.48 [23.32 – 23.59]	Winter et al. 2009
NGC 4138	12 09 29.79	+43 41 07.1	0.0030	Sy1.9	2.62	0.554	22.95 [22.92 – 22.97]	Akylas et al. 2009
NGC 4151	12 10 32.66	+39 24 20.7	0.0033	Sy1.5	30.50	25.00	23.34 [23.08 – 23.56]	Molina et al. 2009
IGR J12107+3822	12 10 44.27	+38 20 10.1	0.0229	Sy1.5	1.47	0.34	22.67 [22.56 – 22.76]	Parisi et al. 2012
IGR J12131+0700	12 12 49.81	+06 59 45.1	0.2095	Sy1.5-1.8	1.74	0.013	20.14	Landi et al. 2007d
NGC4235	12 17 09.91	+07 11 28.3	0.0080	Sy1.2	<0.94	0.28	21.20 [21.18 – 21.23]	Papadakis et al. 2008
Mrk 766	12 18 26.48	+29 48 46.2	0.0129	NLS1	1.81	1.33	<21.95	Turner et al. 2006
NGC 4258	12 18 57.5	+47 18 14.0	0.00149	Sy2	1.69	1.35	23.03 [23.02 – 23.04]	Yamada et al. 2009
4C 04.42	12 22 22.55	+04 13 15.8	0.965	QSO/Blazar	2.30	0.25	20.23	De Rosa et al. 2008
Mrk 50	12 23 24.14	+02 40 44.8	0.0234	Sy1	<1.30	0.98	<21.08	Molina et al. 2009
NGC 4388	12 25 46.93	+12 39 43.3	0.0084	Sy2	24.60	2.30	23.44 [23.42 – 23.45]	Beckmann et al. 2007
NGC 4395	12 25 48.93	+33 32 47.8	0.00106	Sy2	2.090	0.62	22.72 [22.70 – 22.75]	Cappi et al. 2006
IGR J12288+0052	12 28 45.70	+00 50 19.0	0.5756	Sy2	<0.92	0.03	22.40 [21.78 – 22.95]	Fiocchi et al. 2010
3C 273	12 29 06.70	+02 03 08.6	0.1583	Sy1/QSO	19.46	9.62*	20.23	Donato et al. 2005
NGC 4507	12 35 36.55	-39 54 33.3	0.0118	Sy2	16.30	1.28	23.64 [23.58 – 23.63]	Shu et al. 2007
ESO 506-G27	12 38 54.40	-27 18 28.0	0.0250	Sy2	8.32	0.51	23.03 [23.84 – 23.92]	Winter et al. 2008

Name	RA	Dec	z	Class	F_H^\dagger	F_S^\ddagger	$\text{Log } N_H^\circ$	Reference
LEDA 170194	12 39 06.32	-16 10 47.8	0.0367	Sy2	3.77	2.00	22.46 [22.41 - 22.62]	De Rosa et al. 2008
NGC 4593	12 39 39.43	-05 20 39.3	0.009	Sy1	7.12	3.72	20.30	Molina et al. 2009
IGR J12415-5750	12 41 25.74	-57 50 03.5	0.0242	Sy1.5	2.04	0.77	21.48	Molina et al. 2009
IGR J1248.2-5828	12 47 57.84	-58 30 00.2	0.028	Sy1.9	1.02	0.40	22.35 [22.23 - 2.48]	Landi et al. 2010a
NGC 4748	12 52 12.40	-13 24 53.0	0.0146	NLS1	1.27	0.34	20.56	Panessa et al. 2011
ESO 323-32	12 53 20.19	-41 38 07.5	0.016	Sy2	1.81	0.40	25.00 [<i>fixed</i>]	Comastri et al. 2010
3C 279	12 56 11.17	-05 47 21.5	0.5362	QSO/Blazar	2.15	0.60*	20.35	Donato et al. 2005
Mrk 783	13 02 58.84	+16 24 27.5	0.0672	NLS1	2.21	0.65	21.18 [20.84 - 21.38]	Panessa et al. 2011
IGR J13038+5348	13 03 59.43	+53 47 30.1	0.03	Sy1.2	2.74	1.59	20.22	Winter et al. 2009
NGC 4941	13 04 13.08	-05 33 05.7	0.0037	Sy2	1.10	0.07	23.64 [23.49 - 23.84]	Shu et al. 2007
IGR J13042-1020	13 04 14.38	-10 20 22.6	0.0104	Sy2	1.42	0.33	>25.00	Guainazzi et al. 2005a
NGC 4945	13 05 27.28	-49 28 04.4	0.0019	Sy2	25.60	0.54	24.72 [24.64 - 24.75]	Itoh et al. 2008
ESO 323-77	13 06 26.14	-40 24 52.2	0.015	Sy1.2	2.64	0.77	21.54	Malizia et al. 2007
IGR J13091+1137	13 09 05.65	+11 38 01.8	0.0291	XBONG	3.81	0.21	23.63 [23.60 - 23.67]	De Rosa et al. 2012
IGR J13109-5552	13 10 43.35	-55 52 11.4	0.104	Sy1	2.43	0.49	<21.66	Molina et al. 2009
IGR J13149+4422	13 15 17.25	+44 24 25.9	0.0353	Sy2, LINER	2.15	0.75	22.72 [22.62 - 22.83]	Rodriguez et al. 2008
IGR J13168-7157	13 16 54.24	-71 55 27.0	0.0705	Sy1.5	1.08	0.38	21.21	Parisi et al. 2012
IGR J13187+0322 ^(d)	13 18 31.24	+03 19 48.9	0.606	QSO/Blazar?	>1.06	0.015	20.28	Malizia et al. 2011
MCG-03-34-063	13 22 19.06	-16 42 29.6	0.0213	Sy2	2.34	0.21	23.59 [23.48 - 23.72]	Miniutti et al. 2006
Cen A	13 25 27.61	-43 01 08.8	0.0018	Sy2	62.10	21.20	23.17 [23.16 - 23.18]	Markowitz et al. 2007
3C287.1	13 32 53.27	+02 00 45.7	0.2156	Sy1	<2.17	0.28	21.21	Massaro et al. 2010
ESO 383-18	13 33 26.30	-34 00 58.7	0.0124	Sy2	<0.76	0.52	23.29 [23.27 - 23.31]	Noguchi et al. 2009
MCG-06-30-015	13 35 53.80	-34 17 43.8	0.0077	Sy1.2	4.14	3.64	22.17 [22.04 - 22.26]	Molina et al. 2009
NGC 5252	13 38 16.00	+04 32 32.5	0.0230	Sy1.9	4.76	3.00	22.83 [22.78 - 22.92]	Risaliti et al. 2002
IGR J13415+3033	13 41 11.17	+30 22 41.1	0.0398	Sy2	1.85	0.25	23.47 [23.44 - 23.52]	Malizia et al. 2011
IGR J13466+1921	13 46 28.46	+19 22 43.2	0.085	Sy1.2	2.07	0.32	20.27	Parisi et al. 2012
Cen B	13 46 49.04	-60 24 29.3	0.0129	RG/type2	1.13	0.49	22.11 [21.98 - 22.21]	Tartarus Database
4U 1344-60	13 47 36.00	-60 37 03.8	0.013	Sy1.5	7.23	3.57	23.67 [23.41 - 23.90]	Molina et al. 2009
IC 4329A	13 49 19.29	-30 18 34.4	0.0160	Sy1.2	20.90	10.40	21.54 [20.53 - 21.56]	Molina et al. 2009
1AXG J135417-3746	13 54 16.10	-37 46 43.0	0.0509	Sy1.9	1.42	0.34	22.80 [22.69 - 22.90]	Tartarus Database
IGR J13550-7218	13 55 11.45	-72 18 51.3	0.071	Sy2	1.49	0.22	23.28 [23.04 - 23.43]	Rodriguez et al. 2010
IGR J14080-3023	14 08 06.57	-30 23 52.6	0.0237	Sy1.5	1.89	0.64	20.56	Landi et al. 2010a
Circinus Galaxy	14 13 08.90	-65 20 27.0	0.0014	Sy2	20.20	1.00	24.60 [24.56 - 24.67]	Bassani et al. 1999a
NGC 5506	14 13 14.87	-03 12 27.0	0.0062	Sy2	14.90	8.38	22.53 [22.51 - 22.56]	Bassani et al. 1999a
IGR J14175-4641	14 17 03.94	-46 41 39.1	0.076	Sy2	1.62	0.095	23.88 [23.55 - 24.55]	Malizia et al. 2011
NGC 5548	14 17 59.51	+25 08 12.5	0.0172	Sy1.5	3.00	5.30	20.19	Shinozaki et al. 2006
ESO 511-G030	14 19 22.44	-26 38 40.8	0.0224	Sy1	3.42	1.30	20.70	Tartarus Database
H 1419+480	14 21 29.25	+47 47 21.4	0.0723	Sy1.5	<1.76	0.70	20.83	Shinozaki et al. 2006
H 1426+428	14 28 32.57	+42 40 24.8	0.1291	BL Lac	1.79	3.38	21.01 [20.97 - 21.04]	Winter et al. 2009
IGR J14301-4158	14 30 12.17	-41 58 31.4	0.0039	Sy2	0.92	0.27	22.08 [21.95 - 22.34]	Malizia et al. 2011
NGC 5643	14 32 40.70	-44 10 28.0	0.0040	Sy2	1.10	0.084	23.85 [23.70 - 23.95]	Guainazzi et al. 2004
NGC 5728	14 42 23.90	-17 15 11.0	0.0093	Sy2	5.38	0.15	24.14 [24.09 - 24.18]	Comastri et al. 2010
IGR J14471-6414	14 46 28.26	-64 16 24.3	0.053	Sy1.2	1.11	0.48	21.60 [21.43 - 21.73]	Landi et al. 2007d

Name	RA	Dec	z	Class	F_H^\dagger	$F_S^{\dagger\dagger}$	$\text{Log } N_H^\circ$	Reference
IGR J14471-6319	14 47 14.88	−63 17 19.2	0.038	Sy2	1.36	0.39	22.39 [21.83 – 22.65]	Malizia et al. 2007
IGR J14515-5542	14 51 33.13	−55 40 38.4	0.018	Sy2	2.08	0.53	21.52 [21.40 – 21.70]	De Rosa et al. 2011
IGR J14552-5133	14 55 17.80	−51 34 17.0	0.016	NLS1	1.45	0.96	21.53	Panessa et al. 2011
IGR J14561-3738	14 56 08.43	−37 38 52.4	0.024	Sy2	1.55	0.002	>24	Sazonov et al. 2008
IC 4518A	14 57 41.16	−43 07 55.2	0.0163	Sy2	2.08	0.29	23.15 [23.11 – 23.23]	De Rosa et al. 2008
MKN 841	15 04 01.20	+10 26 16.1	0.0364	Sy1.5	<3.40	1.62	20.84	Piconcelli et al. 2005
IRAS 15091-2107	15 11 59.80	−21 19 02.0	0.0446	NLS1	2.44	0.90	21.15 [21.00 – 21.25]	Panessa et al. 2011
SWIFT J1513.8-8125	15 14 41.92	−81 23 38.9	0.06836	Sy1.2	1.83	1.11	21.88 [21.61 – 22.00]	Parisi et al. 2012
IGR J15161-3827	15 15 59.70	−38 25 46.8	0.0365	Sy2	<6.22	0.12	23.34 [23.11 – 23.59]	Rodriguez et al. 2009
IGR J15311-3737	15 30 51.79	−37 34 57.3	0.127	Sy1	0.89	1.86	21.32	Malizia et al. 2011
NGC 5995	15 48 24.95	−13 45 28.0	0.0252	Sy1.9	3.47	2.20	21.93 [21.75 – 22.10]	Shu et al. 2007
IGR J15539-6142	15 53 35.28	−61 40 58.4	0.015	Sy2	1.58	0.073	23.24 [22.66 – 23.70]	Malizia et al. 2007
IGR J15549-3740	15 54 46.76	−37 38 19.1	0.019	Sy2	1.72	0.34	22.76 [22.58 – 22.85]	Malizia et al. 2011
IGR J16024-6107	16 01 48.23	−61 08 54.7	0.011	Sy2	0.92	0.30	21.40 [21.38 – 21.45]	De Rosa et al. 2012
IGR J16056-6110	16 05 51.17	−61 11 44.0	0.052	Sy1.5	1.30	0.14	21.31	Landi et al. 2007a
IGR J16119-6036	16 11 51.36	−60 37 53.1	0.016	Sy1.5	2.53	0.33	21.36	Molina et al. 2009
IGR J16185-5928	16 18 36.44	−59 27 17.4	0.035	NLS1	1.55	0.27	23.02 [22.71 – 23.42]	Panessa et al. 2011
IGR J16351-5806	16 35 13.17	−58 04 49.7	0.0091	Sy2	1.96	0.031	24.68 [24.50 – 25.09]	Malizia et al. 2009
IGR J16385-2057	16 38 30.91	−20 55 24.6	0.0269	NLS1	1.27	0.53	21.08	Panessa et al. 2011
IGR J16426+6536	16 43 04.07	+65 32 50.9	0.323	NLS1	3.45	0.0085	20.41	Malizia et al. 2011
IGR J16482-3036	16 48 15.20	−30 35 03.7	0.0313	Sy1	<3.85	2.00	21.00 [20.48 – 21.20]	Molina et al. 2009
SWIFT J1650.5+0434	16 50 42.70	+04 36 18.0	0.0321	Sy2	2.19	0.32	22.68 [22.54 – 22.79]	Malizia et al. 2011
ESO 138-1 ^(e)	16 51 20.21	−59 14 04.2	0.0091	Sy2	1.06	0.180	>24.18	Collinge et al. 2000
NGC 6221 ^(e)	16 52 46.32	−59 13 00.8	0.005	Sy2	1.06	1.41	22.04 [22.00 – 22.07]	Panessa et al. 2002
NGC 6240	16 52 58.97	+02 24 01.7	0.0245	Sy2, LINER	5.42	0.20	24.30 [24.28 – 24.38]	Vignati et al. 1999
Mrk 501	16 53 52.22	+39 45 36.6	0.0337	BL Lac	4.32	16.7**	20.07	Donato et al. 2005
IGR J16558-5203	16 56 05.62	−52 03 40.9	0.054	Sy1.2	2.89	1.75	23.48 [23.28 – 23.61]	Panessa et al. 2008
SWIFT J1656.3-3302	16 56 16.85	−33 02 11.1	2.4	QSO/Blazar	3.04	0.44	21.34	Masetti et al. 2008a
IGR J17009+3559	17 00 53.00	+35 59 56.2	0.113	XBONG	2.13	0.11	23.37 [23.07 – 23.60]	Parisi et al. 2012
IGR J17036+3734	17 03 20.20	+37 37 24.9	0.065	Sy1	2.01	0.21	20.39	Malizia et al. 2011
NGC 6300	17 16 59.47	−62 49 14.0	0.0037	Sy2	6.51	0.86	23.38 [23.34 – 23.40]	Matsumoto et al. 2004
MCG+08-31-041	17 19 14.45	+48 58 49.6	0.0242	Sy1, LINER	7.66	1.10	<21.22	Tartarus Database
GRS 1734-294	17 37 28.35	−29 08 02.5	0.0214	Sy1	8.25	3.84	>21.32	Molina et al. 2009
2E 1739.1-1210	17 41 55.25	−12 11 56.6	0.037	Sy1.2	2.89	1.29	21.18 [21.08 – 21.25]	Molina et al. 2009
IGR J17476-2253	17 47 29.71	−22 52 44.3	0.0463	Sy1	1.81	0.26	21.48	Malizia et al. 2011
IGR J17488-3253	17 48 55.13	−32 54 52.1	0.02	Sy1	3.96	1.40	21.53 [21.52 – 21.54]	Molina et al. 2009
IGR J17513-2011	17 51 13.62	−20 12 14.6	0.047	Sy1.9	2.43	0.58	21.82 [21.81 – 21.83]	De Rosa et al. 2012
1RXS J175252.0-053210	17 52 52.00	−05 32 10.0	0.136	Sy1.2	1.00	0.26	21.33	Malizia et al. 2011
IGR J18027-1455	18 02 47.37	−14 54 54.8	0.035	Sy1	3.85	0.66	21.48 [21.34 – 21.58]	Molina et al. 2009
IGR J18218+6421	18 21 57.24	+64 20 36.2	0.297	Sy1.2	1.73	1.24	20.54	Jimenez-Bailon et al. 2007
IGR J18244-5622	18 24 19.39	−56 22 09.1	0.0169	Sy2	2.66	0.67	23.15 [22.79 – 23.47]	Malizia et al. 2007
IGR J18249-3243	18 24 55.92	−32 42 57.7	0.355	Sy1/QSO	1.02	0.52	21.14	Landi et al. 2007b

Name	RA	Dec	z	Class	F_H^\dagger	$F_S^{\dagger\dagger}$	$\text{Log } N_H^\circ$	Reference
IGR J18259-0706 ^(f)	18 25 57.58	-07 10 22.8	0.037	Sy1	1.36	0.54	21.91 [21.87 – 21.93]	this work
IGR J18311-3337	18 31 14.75	-33 36 08.5	0.0687	Sy2	1.66	0.026	22.15 [21.60 – 22.81]	Malizia et al. 2011
PKS 1830-211	18 33 39.92	-21 03 39.9	2.507	QSO/Blazar	4.83	1.00	22.29 [22.23 – 22.35]	De Rosa et al. 2005
3C382	18 35 03.39	+32 41 46.8	0.0579	Sy1	5.91	5.98	20.79	Grandi et al. 2006
ESO 103-35	18 38 20.30	-65 25 41.0	0.0133	Sy2	8.15	2.40	23.30 [23.25 – 23.29]	De Rosa et al. 2011
3C 390.3	18 42 08.99	+79 46 17.1	0.0561	Sy1.5	6.13	2.14	20.63	Molina et al. 2009
ESO 140-43	18 44 54.01	-62 21 53.2	0.0142	Sy1.5	3.93	9.50	23.04 [22.70 – 23.15]	Ricci et al. 2010
IGR J18470-7831	18 47 02.83	-78 31 49.5	0.0743	Sy1	1.83	0.80	20.08 [19.30 – 20.43]	Shinozaki et al. 2006
ESO 25-2	18 54 40.39	-78 53 54.4	0.0292	Sy1	2.15	0.20	20.92	Malizia et al. 2011
2E 1853.7+1534	18 56 00.00	+15 38 13.0	0.084	Sy1	2.36	1.22	<21.59	Molina et al. 2009
2E 1849.2-7832	18 57 07.68	-78 28 21.3	0.0420	Sy1	3.27	0.77	20.92	Tartarus Database
IGR J19077-3925	19 07 50.36	-39 23 31.9	0.076	Sy1.9	1.49	0.36	21.15 [20.78 – 21.38]	Malizia et al. 2011
IGR J19118-1707	19 11 42.64	-17 10 05.1	0.0234	LINER	<1.17	0.14	23.02 [22.74 – 23.27]	Malizia et al. 2011
PKS 1916-300	19 19 28.01	-29 58 09.7	0.1668	Sy1.5-1.8	<1.23	0.62	20.90	Malizia et al. 2011
ESO 141-G055	19 21 14.13	-58 40 13.3	0.0371	Sy1.2	4.65	2.45	20.68	Dadina 2007
1RXS J192450.8-291437	19 24 51.06	-29 14 30.1	0.352	BL Lac	1.43	0.81	20.86 [20.63 – 21.01]	Malizia et al. 2011
SWIFT J1930.5+3414	19 30 13.81	+34 10 49.8	0.0629	Sy1.5-1.8	1.73	0.22	23.44 [23.14 – 23.68]	Winter et al. 2009
QSO B1933-400	19 37 16.22	-39 58 01.5	0.9655	QSO/Blazar	1.32	0.19	21.11 [20.48 – 21.41]	Malizia et al. 2011
IGR J19378-0617	19 37 33.00	-06 13 05.0	0.0106	NLS1	1.83	2.70	23.50 [23.38 – 23.63]	Panessa et al. 2011
IGR J19405-3016	19 40 15.07	-30 15 52.2	0.052	Sy1.2	<1.47	0.11	20.96	Landi et al. 2007b
NGC 6814	19 42 40.40	-10 19 24.0	0.0052	Sy1.5	5.66	0.17	21.10	Molina et al. 2009
XSS J19459+4508	19 47 32.88	+44 52 58.8	0.0539	Sy2	1.98	0.41	23.04 [23.00 – 23.08]	Sazonov et al. 2005
IGR J19491-1035	19 49 08.69	-10 34 34.5	0.0246	Sy1.2	1.33	0.56	22.26 [22.03 – 22.41]	Malizia et al. 2011
3C 403	19 52 15.82	+02 30 24.3	0.059	Sy2	2.02	1.30	23.65 [23.58 – 23.62]	Kraft et al. 2005
Cyg A	19 59 28.36	+40 44 02.1	0.0561	Sy2	8.34	1.20	23.30 [23.25 – 23.32]	Young et al. 2002
ESO 399-20	20 06 57.95	-34 32 54.6	0.0249	NLS1	1.75	0.13	20.85	Panessa et al. 2011
NGC 6860	20 08 46.90	-61 06 01.0	0.01488	Sy1.5	3.90	1.80	21.00 [21.23 – 21.63]	Winter et al. 2008
IGR J20186+4043	20 18 38.71	+40 41 00.3	0.0144	Sy2	2.30	0.28	22.76 [22.72 – 22.80]	De Rosa et al. 2012
IGR J20216+4359	20 21 49.04	+44 00 39.4	0.017	Sy2	1.32	0.56	23.11 [23.04 – 23.18]	Bikmaev et al. 2008
IGR J20286+2544(1) ^(g)	20 28 35.10	+25 43 59.5	0.0139	Sy2/SB	3.34	2.11	23.78 [23.61 – 23.92]	Rodriguez et al. 2009
IGR J20286+2544(2) ^(g)	20 28 28.90	+25 43 24.6	0.0144	XBONG	1.28	<1.6	23.97 [23.52 – 24.23]	Rodriguez et al. 2009
4C 74.26	20 42 37.18	+75 08 02.5	0.104	Sy1	4.27	2.53	21.15 [21.04 – 21.20]	Molina et al. 2009
SWIFT J2044.0+2832	20 44 04.00	+28 33 03.0	0.05	Sy1	2.62	0.71	21.24	Malizia et al. 2011
Mrk 509	20 44 09.77	-10 43 24.4	0.0344	Sy1.5	7.63	3.4	20.63	Shinozaki et al. 2006
IGR J20450+7530	20 44 34.49	+75 31 58.9	0.095	Sy1	<3.57	0.032*	21.20 [20.86 – 21.45]	Landi et al. 2010b
S52116+81	21 14 00.00	+82 04 47.0	0.084	Sy1	<2.76	1.21	21.38	Molina et al. 2009
1RXS J211928.4+333259	21 19 29.13	+33 32 57.0	0.051	Sy1.5	1.55	0.59	21.52 [21.59 – 21.73]	Malizia et al. 2011
IGR J21247+5058	21 24 39.33	+50 58 26.0	0.020	Sy1	12.60	4.88	22.89 [22.79 – 22.99]	Molina et al. 2009
SWIFT J2127.4+5654	21 27 45.58	+56 56 35.6	0.0147	NLS1	3.14	4.2	21.90	Panessa et al. 2011
RX J2135.9+4728	21 35 54.2	+47 28 22.3	0.025	Sy1	1.79	0.62	20.30 [21.46 – 21.78]	Winter et al. 2009
1RXS J213944.3+595016	21 39 45.10	+59 50 14.0	0.114	Sy1.5	1.02	0.59	21.54 [21.15 – 21.86]	Landi et al. 2010a
PKS 2149-306	21 51 55.52	-30 27 53.7	2.345	QSO/Blazar	2.51	0.80	20.34	Elvis et al. 2000
IGR J21565+5948	21 56 04.20	+59 56 04.5	0.208	Sy1	0.98	0.12	21.81	Landi et al. 2010c
Mrk 520	22 00 41.37	+10 33 08.7	0.0266	Sy1.9	4.13	0.63	22.63 [22.26 – 22.49]	Winter et al. 2009

Name	RA	Dec	z	Class	F_H^\dagger	$F_S^{\dagger\dagger}$	$\text{Log } N_H^\circ$	Reference
NGC 7172	22 02 01.90	−31 52 11.6	0.0087	Sy2	7.93	4.30	22.86 [22.85 – 22.87]	De Rosa et al. 2012
BL Lac	22 02 43.29	+42 16 40.0	0.686	BL Lac	2.40	2.02	21.44	Donato et al. 2005
IGR J22292+6647	22 29 13.84	+66 46 51.5	0.112	Sy1.5	1.11	0.69	21.68	Landi et al. 2010a
NGC 7314	22 35 46.23	−26 03 00.9	0.0048	Sy1.9	3.02	1.91	22.02 [21.95 – 22.07]	Dewangan et al. 2005
IGR J22367-1231	22 36 46.49	−12 32 42.6	0.0241	Sy1.9	2.76	1.09	22.42 [22.32 – 22.53]	Malizia et al. 2011
3C 452	22 45 49.10	+39 41 15.0	0.0811	Sy2	3.00	0.50	23.77 [23.70 – 23.83]	Isobe et al. 2002
IGR J22517+2218	22 51 53.50	+22 17 37.3	3.668	QSO/Blazar	3.15	0.26	22.48 [22.00 – 22.70]	Bassani et al. 2007
3C 454.3	22 53 57.75	+16 08 53.6	0.859	QSO/Blazar	19.17	6.10	21.28 [20.78 – 21.53]	Ghisellini et al. 2007
QSO B2251-178	22 54 05.88	−17 34 55.3	0.0640	Sy1.2	6.66	2.00	22.33 [21.97 – 22.44]	Molina et al. 2009
NGC 7465	23 02 00.95	+15 57 53.6	0.0066	Sy2, LINER	2.62	0.41	23.66 [23.43 – 23.87]	Guainazzi et al. 2005b
NGC 7469	23 03 15.75	+08 52 25.9	0.0163	Sy1.5	4.49	2.30	20.46	Shinozaki et al. 2006
MCG-02-58-022	23 04 43.48	−08 41 08.6	0.0469	Sy1.5	4.30	3.18	20.56	Molina et al. 2009
NGC 7582	23 18 23.49	−42 22 14.1	0.0052	Sy2	<2.80	0.23	24.04 [23.87 – 24.26]	Piconcelli et al. 2007
IGR J23206+6431	23 20 36.58	+64 30 45.2	0.0717	Sy1	<0.66	0.55	21.95 [21.30 – 22.28]	Rodriguez et al. 2009
IGR J23308+7120	23 30 37.68	+71 22 46.6	0.037	Sy2 ?	<0.53	0.14	22.96 [22.90 – 23.03]	De Rosa et al. 2012
IGR J23524+5842	23 52 22.11	+58 45 30.7	0.164	Sy2 ?	1.23	0.28	22.46 [22.41– 22.52]	De Rosa et al. 2012